Significant role of biomass burning in heavy haze formation in Nanjing, a megacity in China: Molecular-level insights from intensive $PM_{2.5}$ sampling on winter hazy days

Mingjie Kang[1,2], Mengying Bao[1,2,3], Wenhuai Song[1,2], Aduburexiati Abulimiti[1,2], Changliu Wu[1,2], Fang Cao[1,2], Sönke Szidat[4], Yanlin Zhang[1,2]

[1] School of Ecology and Applied Meteorology, Nanjing University of Information Science and Technology. Nanjing 210044, China.

[2] Atmospheric Environment Center, Joint Laboratory for International Cooperation on Climate and Environmental Change, Ministry of Education, Nanjing University of Information Science and Technology. Nanjing 210044, China.

[3] Huzhou Meteorological Administration, Huzhou, 313000, China

[4] Department of Chemistry, Biochemistry and Pharmaceutical Sciences & Oeschger Centre for Climate Change Research, University of Bern, Bern, 3012, Switzerland

Correspondence to: Yanlin Zhang (zhangyanlin@nuist.edu.cn; dryanlinzhang@outlook.com)

Abstract. Reports on molecular-level characterization of primary and secondary constituents in $PM_{2.5}$ at high time resolution are limited to date, especially during haze events. The study explored molecular composition and source contributions of $PM_{2.5}$ with comprehensive analytical methods by conducting intensive sampling at roughly 2-hour intervals during hazy days in winter. Results show that organic matters were the predominant species, followed by NO_3^-. Biomass burning (BB) was the biggest contributor to organic carbon (OC), both in concentration and in proportion. Radiocarbon analysis of carbonaceous fractions reflects that fossil fuels dominate water-soluble organic carbon (WSOC) (61-82%) likely resulting from increased coal combustion for residential cooking and heating and the coal-fired industry in cold times. Interestingly, the contribution of non-fossils instead of fossil fuels to WSOC enhanced with aggravating haze pollution, coinciding with significantly intensified BB during that time. Other non-fossil sources, including fungal spores and plant debris, showed a larger contribution to OC in light haze episodes. For secondary sources, naphthalene-derived secondary organic carbon (SOC) contributed more to OC in $PM_{2.5}$ (0.27-2.46%) compared to biogenic emissions (0.05-1.10%), suggesting fossil fuels may dominate SOC formation during urban haze events. SOC declined with rising haze pollution and presented high levels on days with high temperature and low relative humidity due to elevated photooxidation. Additionally, BB can raise secondary formation as well as the emissions of other sources, as demonstrated by the significant relationships between BB tracers and many other source tracers. These findings illustrate that BB likely plays a significant role in the heavy winter haze.

1. Introduction

The air quality of China has improved a lot over the past decade due to extensive implementation of emission controls across the country. However, such progress was unexpectedly shattered by severe air pollution happening during COVID-19 lockdown when anthropogenic emissions significantly decreased (Huang et al., 2020b; Le et al., 2020; Wang et al., 2020). This underscores the ongoing challenge of controlling $PM_{2.5}$ pollution, especially during cold seasons in megacities. Additionally, the emergence of ozone (O_3) pollution in many urban areas complicates the situation. Rising O_3 levels, associated with increased atmospheric oxidation capacity (Kang et al., 2021), create more complex air pollution scenarios due to intricate secondary aerosol formations and the combined effects of $PM_{2.5}$ and O_3.

$PM_{2.5}$ exerts influences on air visibility, regional/global radiation balance, hydrological cycle (Kaufman et al., 2002), and human and ecosystem health (Alexeeff et al., 2023; Chen et al., 2022; Pope et al., 2004; Wang et al., 2022). In response scientists have carried out a series of studies to analyze aerosol components and emission sources (Cheng et al., 2016; Huang et al., 2014, 2020b, a; Jimenez et al., 2009; Kang et al., 2016, 2018a, b, 2019; Li et al., 2016a; Liu et al., 2014; Sun et al., 2014; Wang et al., 2006; Yang et al., 2024; Zhang et al., 2012, 2018). These studies revealed that $PM_{2.5}$ pollution is formed through mixed interaction of primary and secondary sources, including anthropogenic and biogenic origins. Primary sources mainly contain plant emissions, fungal spores, soil dust, fossil fuel combustion, and biomass burning (BB) (Anon, 2002; Fu et al., 2012; Kang et al., 2018b, a; Morris et al., 2011; Pöschl et al., 2010; Simoneit, 2002; Zhang et al., 2015, 2016) while secondary sources primarily involve homogeneous and heterogeneous reactions of biogenic and anthropogenic precursors (e.g., NO_x, NH_3, SO_2, and VOCs) (Fu et al., 2010; Huang et al., 2014). Many $PM_{2.5}$ species carry origin information and thus can serve as tracers to determine specific sources.

For example, saccharides (i.e., anhydrosugars, sugars, and sugar alcohols) are important water-soluble organic constituents of aerosols (Simoneit et al., 2004b; Sindelarova et al., 2014), which can be cloud condensation nucleus and ice nuclei thus influencing Earth's climate and water supply (Kaufman et al., 2002). Among them, levoglucosan is widely used as a typical BB tracer (Elias et al., 2001; Li et al., 2021b; Liu et al., 2013). BB has a substantial impact on the

secondary organic aerosols (SOA) budget and climate change (Chen et al., 2017b; Zhang et al., 2024). For example, substituted phenols from lignin combustion, which serve as BB tracers as well, undergo aqueous phase oxidation with photooxidants to form SOA, significantly influencing the evolution of organic aerosols (Zhang et al., 2024). However, the contribution of BB emissions to SOA formation is not yet well understood and is consequently not accurately represented in regional and global atmospheric chemistry models. Sugar alcohols like arabitol and mannitol can be utilized to assess the contribution of airborne fungal spores to carbonaceous aerosols (Bauer et al., 2008a, b; Fu et al., 2012, 2016). Other primary sugars (e.g., glucose) are useful markers for plant pollen, fruits, and detritus (Fu et al., 2016; Puxbaum and Tenze-Kunit, 2003).

Secondary organic aerosols (SOA) are also a significant fraction, produced by the reactions of oxidants (e.g., OH) with biogenic/anthropogenic VOCs (Claeys et al., 2004; Hallquist et al., 2009; Huang et al., 2014; Mozaffar et al., 2020). Biogenic VOCs, such as isoprene, monoterpenes, and sesquiterpenes, play a vital role in global SOA formation and atmospheric processes (Claeys et al., 2004; Griffin et al., 1999; Guenther et al., 2006; Pöschl et al., 2010; Sindelarova et al., 2014; Zhang et al., 2007), while anthropogenic VOCs (e.g., aromatic hydrocarbons) tend to be more important in populated cities and nearby areas where coal combustion, transportation, solvent use and biofuel/biomass burning contribute significantly (Chen et al., 2017b; Ding et al., 2017; Srivastava et al., 2022). Despite its high importance and wide existence, comprehensive characterization of SOA at the molecular level is difficult because of complex and non-linear reactions and variable meteorological conditions. The lack of molecular-level composition, abundance, and formation mechanisms of SOA at high time resolution introduces inevitable uncertainties in modeling and forecasting air pollutants (Zhang et al., 2022, 2023). Correctly simulating SOA with chemical transport models therefore can become more challenging.

Other than the aforementioned organic species in $PM_{2.5}$, secondary inorganic aerosols (SIA, the sum of sulfate (SO_4^{2-}), nitrate (NO_3^-), and ammonium (NH_4^+)) equally account for a substantial proportion of fine aerosols, especially on heavy pollution days (Fu et al., 2012; Huang et al., 2014; Lu et al., 2019; Yan et al., 2023). Nitrate and sulfate in $PM_{2.5}$ are mostly formed by

secondary formation and are accordingly expected to have significant regional influences once they are emitted, particularly in winter. A recent study reported that nitrate comprised the largest fraction of $PM_{2.5}$ in China during severe haze, and NO_x emission reduction was regarded as an effective measure to combat air pollution (Yan et al., 2023). Nevertheless, this conclusion was challenged by the sustained severe haze during COVID-19 lockdown while NO_x emissions substantially declined (Le et al., 2020), suggesting the complexity of $PM_{2.5}$ pollution and callout of more research work.

Although previous studies over past decades provide valuable information about aerosol components, the molecular-level compositions and concentrations of fine particles still have not been well understood due to their high spatial and temporal variability, especially at sub-daily (hourly) levels. One reason is that aerosol properties can be modified at any time during the transport through dry or wet deposition, in-cloud processes, and atmospheric chemical reactions. Intensive aerosol sampling with high time resolution is then necessary for better quantifying the $PM_{2.5}$ components and source contributions. Former researches mostly focused on analyzing the differences between hazy and clean days while very few reported variations among different hazy days on sub-daily (e.g., hourly) basis in part due to the difficulty in too frequent aerosol samplings. However, these molecular-level data at high time resolution are useful and necessary for exploring the key factors controlling haze formation, which is important for setting up regulatory standards in response to rapid changes in aerosol composition and concentrations through time and place. Furthermore, the impacts of aerosol particles with different properties (e.g., chemical composition) on climate (Kanakidou et al., 2005; Kawana et al., 2022) remain unclear, and molecular-level $PM_{2.5}$ components at hourly intervals would greatly help better understand such issues.

Herein, we systematically unraveled hourly variation in molecular-level $PM_{2.5}$ components during haze events in Nanjing, a major city of the Yangtze River Delta with concentrated heavy industry and population. Concentrations of major organic and inorganic components such as BB tracers, sugar and sugar alcohols, oxidation products (e.g., biogenic SOA tracers and aromatic acids), and water-soluble icons were measured and compared across three different haze pollution levels. Contributions of primary sources to organic carbon (OC) in $PM_{2.5}$ samples

were estimated including BB, fungal spores, and plant debris. Contributions of secondary OC formed by biogenic and anthropogenic VOCs to total OC were also calculated. ^{14}C measurement were performed on water-soluble organic carbon (WSOC) to accurately quantify the contribution of fossil fuel sources. The molecular-level results of $PM_{2.5}$ components and source contributions at high time resolution will help understand the haze formation and evolution in megacities.

2. Materials and methods

2.1 Sampling

The sampling site was located on the rooftop of a building at the Nanjing University of Information Science and Technology in Nanjing, China (32.2°N, 118.72°E). A total of 23 $PM_{2.5}$ samples were collected onto Prebaked quartz fiber filters (Pallflex) at a roughly 2-hour interval from 31 December 2017 to 2 January 2018. High-volume air sampler (KC-1000, Qingdao Laoshan Electric Inc., China) was used at a flow rate of 1.05 m^3 min^{-1}. The field blank was also collected with pump off during sampling. All the samples were stored in darkness at −20°C for later analysis. In this study, the whole sampling period was divided into three episodes according to $PM_{2.5}$ levels, i.e., > 200, 100–200, and <100 μg m^{-3}, representing a haze pollution process from heavily polluted days to moderately polluted days.

2.2 Measurements of organic molecules

Sugar compounds, including anhydrosugars, sugar alcohols, and sugars, were measured using ion chromatography (Dionex ICS-5000+, ThermoFisher Scientific, USA) after being extracted with ultra-pure water (Milli-Q Reference, America). Standard curves establishment and blank correction were conducted during the analysis. Other organic compounds, including biogenic SOA tracers (isoprene, sesquiterpene, and monoterpene), diacids, and other main organic molecules appeared in the present study were determined by gas chromatography/mass spectrometry (Agilent Technologies; Santa Clara, CA). The average recoveries ranged from 70% to 110% and repeatability experiments showed that the deviation was less than 15%. All the data were corrected with field blanks. More details about measurements can be found in previous studies (Bao et al., 2023). The total mass concentrations of SOC produced by isoprene

(2-methylglyceric acid and 2-methyltetrols were used), α/β-pinene, and β-caryophyllene were estimated using the tracer-based method by Kleindienst et al. (2007). The BB derived OC and fungal-spore derived OC were calculated using the methods in earlier reports (Bauer et al., 2008a; Fu et al., 2014).

2.3 Measurements of OC, EC, WSOC, and inorganic icons

The elemental and organic carbon content were detected using a Sunset Lab EC/OC Analyzer with the Interagency Monitoring of Protected Visual Environments (IMPROVE) 7-step program heating method. This approach has been proved to be more accurate for EC and OC measurement (Wu et al., 2020). Details about determination of water-soluble OC (WSOC) can be found elsewhere (Bao et al., 2022). The water-soluble ions were measured by ion chromatography (IC), and more detailed information is provided elsewhere (Bao et al., 2023). The detected inorganic icons are listed in Table 1.

2.4 ^{14}C analysis of the carbonaceous fractions

The ^{14}C of WSOC was determined by extracting WSOC using deionized water and then collecting the extracted solution for ^{14}C measurement using chemical wet oxidation of the water extraction eluate (Song et al., 2022). The ^{14}C results are expressed as the fractions of measured carbon, which is calculated as below (F^{14}C):

$$F^{14}C = \frac{(^{14}C/^{12}C)_{sample}}{(^{14}C/^{12}C)_{1950}} \quad (1)$$

Where $(^{14}C/^{12}C)_{1950}$ is the reference isotopic ratio in 1950. Then, these $F^{14}C$ values were corrected by dividing by the reference value ($f_{nf,ref}$) to remove potential impacts of nuclear bomb tests in the 1950s and 1960s, in order to obtain the non-fossil fractions of WSOC. More details can be found in papers by Song et al. (2022) and Zhang et al. (2017).

$$f_{nf} = F^{14}C / f_{nf,ref} \quad (2)$$

2.5 Backward trajectories below 500 m above ground level

Since regional transport also imposes influences on $PM_{2.5}$ levels (Chang et al., 2019; Chen et al., 2017a), the Hybrid Single-Particle Lagrangian Integrated Trajectory (HYSPLIT) model was employed to compute backward trajectories of air masses arriving at the sampling site to

estimate the impacts of air pollution transport on haze formation (available at https://www.ready.noaa.gov/hypub-bin/trajtype.pl?runtype=archive). MODIS active fire/hotspot products were utilized to evaluate the impact of open biomass burning during the entire sampling period. Based on the backward trajectory analysis, the air masses throughout the sampling period were significantly influenced by biomass burning, as illustrated in Fig. S1. By comparison, the third episode showed a greater influx of clean ocean air masses (Fig. S1c).

3. Results and discussion

3.1 Inorganic icons

Table 1 lists the concentrations of identified inorganic icons, in which Cl^-, NO_3^-, SO_4^{2-}, and NH_4^+ are the major inorganic components during the entire sampling period. The contribution of SIA to total $PM_{2.5}$ far exceeded that of organic matters (OM) during all haze episodes, suggesting SIA contributes greatly to the occurrence of heavy haze. As illustrated in Figure 1, NO_3^- was found to be the second dominant species (20.1–25.6%) in $PM_{2.5}$ next to organic matters (OM), particularly in the heaviest haze event, consistent with the findings in a megacity of Canada (Rivellini et al., 2024). However, these percentages are greater than those in other megacities reported by Huang et al. (2014) (7.1–13.6%). Such discrepancy may be caused by the spatial-temporal variations in energy mix and meteorological parameters over years. The predominance of NO_3^- in SIA (30–52%) is in agreement with the study about nitrate aerosols over another megacity in China (~ 43%) (Fan et al., 2020). The major sources of NO_3^- include vehicles, coal combustion, natural gas burning and biomass burning (Fan et al., 2023; Lin et al., 2024; Zhang et al., 2014a). The rising NO_3^- relative to SO_4^{2-} may be associated with the decline in SO_2 and the rise in NH_3 emissions in recent years, which allows more HNO_3 to condense into particulate NO_3^- (Shah et al., 2024), as indicated by the significant relationship between NO_3^- and NH_4^+ ($r = 0.98$, $p < 0.01$). Higher concentration (56.0 ± 4.4 μg m^{-3}) and contribution (~ 25.6%) of NO_3^- appeared in the highest-$PM_{2.5}$ episode. This is probably related to the high relative humidity (RH) in this period (Fig. S2), which usually comes with high aerosol liquid water content (Bian et al., 2014) and accordingly leads to more

heterogeneous reactions of nitrate formation (Lin et al., 2020). On the other hand, the relatively colder temperatures in heavy haze episode favor the partitioning of HNO_3 from the gas phase to the particle phase. NO_3^- was also significantly correlated with non-sea-salt SO_4^{2-} (nss-SO_4^{2-}, calculated by subtracting sea-salt sulfate from the total sulfate using the typical sulfate-to-sodium mass ratio of 0.252 in seawater (Yang et al., 2015)) ($r = 0.92$, $p < 0.01$), suggesting they may share similar sources or formation pathways (Zhang et al., 2014a). Actually, under polluted conditions with high RH, reactive nitrogen chemistry in aerosol water is a source of SO_4^{2-}, where NO_x is not only a precursor of nitrate but also an important oxidant for sulfate formation (Cheng et al., 2016). Therefore, NO_x emission reductions have great potential in effectively reducing atmospheric sulfate, nitrate, and even O_3 pollution simultaneously (Kang et al., 2021; Shah et al., 2024). Interestingly, these three SIA components (NO_3^-, SO_4^{2-}, and NH_4^+) were observed to be strongly correlated with BB tracers (e.g., levoglucosan and mannosan), with $p < 0.01$ and r in the range of 0.63–0.80, indicating BB was able to promote the secondary production of SIA significantly. Given that the precursors of NO_3^- and SO_4^{2-}, i.e., NO_x and SO_2, are mainly contributed by fossil fuel combustion activities (e.g., transportation and industrial emissions) in urban areas, the above relationships thus suggest that BB may contribute greatly to the secondary transformation of fossil-fuel-derived precursors.

3.2 OC, EC, WSOC, and ^{14}C of WSOC

Similarly, the abundance of EC, OC, WSOC, and WISOC decreased with decreasing $PM_{2.5}$ levels (Table 1), in line with growing wind speeds. Compared with other episodes, the first episode with $PM_{2.5} > 200$ μg m^{-3} had relatively high RH, low temperature, and low wind speed (Fig. S2), demonstrating adverse meteorological conditions boost haze formation. As displayed in Table 1, the mass concentrations of OC and EC were in the range of 8.74–41.1 and 1.26–3.08 μg m^{-3}, respectively. Such OC values are similar to those previously reported in $PM_{2.5}$ aerosols over Nanjing while EC levels are lower (Li et al., 2015, 2016b), reflecting the reduction of primary emissions as a result of tightened emission controls over past years. OC and EC are significantly correlated ($r = 0.87$, $p < 0.01$, Fig. S3), suggesting they may share common sources,

such as BB, vehicle exhaust, and fossil fuel combustion (Ji et al., 2019). OC/EC ratios showed an increasing trend with rising $PM_{2.5}$ levels (from an average of 8.7 to 13.3) (Table 1 and Fig. 2), close to those in regions dominated by BB (Boreddy et al., 2018; Zhang et al., 2014b). It was reported that BB tended to emit relatively high fractions of OC rather than EC (Andreae and Merlet, 2001), thus the high OC/EC ratios in this study illustrate substantial contributions from BB, particularly during heavy haze events. In addition, high OC/EC ratios observed in this study (> 2.0–2.2) indicate the presence of secondary organic aerosol (Li et al., 2016b). This may be partially attributed to BB, which is a significant source of oxidants (Chang et al., 2024) and an important contributor to SOA formation (Li et al., 2024; Lim et al., 2019; Yee et al., 2013).

OC can be divided into water-soluble organic carbon (WSOC), which is often composed of BB-derived and aged OC, and water-insoluble organic carbon (WISOC), normally representing primary OC (Zhang et al., 2014b). As shown in Fig. 2, WISOC concentration (4.55–25.8 μg m^{-3}) is on average higher than WSOC, becoming the major portion of OC. WSOC ranged from 3.84 to 18.1 μg m^{-3} with higher values occurring in the most $PM_{2.5}$ polluted episode (14.3 ± 2.62 μg m^{-3}), comparable to the numbers previously reported in winter (14.0 μg m^{-3}) (Li et al., 2018). The ratios of WSOC/OC were relatively higher in more polluted periods ($PM_{2.5}$ > 100 μg m^{-3}) with an average of 0.40 ± 0.06 and 0.43 ± 0.03, respectively (Table 1). It was reported that higher WSOC/OC ratios (> 0.4) indicate the significant contribution of secondary organic aerosol and aged aerosols (Boreddy et al., 2018; Ram et al., 2010). Considering the high RH in the most polluted episode, the aqueous-phase oxidations of anthropogenic and/or biogenic VOCs may be partially responsible for more WSOC formation during this period (Youn et al., 2013). In comparison, the lower WSOC/OC ratios (0.35 ± 0.17) in the third episode ($PM_{2.5}$ < 100 μg m^{-3}) likely suggest rising primary emissions containing large amounts of water-insoluble organics (e.g., lipid compounds), as indicated by greater WISOC/OC ratios during this period (0.65 ± 0.17). In addition to secondary formation, WSOC was also found to be significantly correlated with levoglucosan ($r = 0.74$, $p < 0.01$), indicating BB was an important contributor to WSOC. Soluble organic gases derived from BB, such as phenols, can react with oxidants in the aqueous phase to form SOA in aerosol liquid water and clouds, significantly contributing to

SOA formation. Moreover, this aqueous SOA formation greatly increases as relative humidity (RH) increases (Zhang et al., 2024). Given the high relative humidity during the most polluted periods, aqueous SOA production from BB-derived organic gases mostly likely play a crucial role in heavy haze formation. Aqueous SOA generation from BB emissions was also confirmed by many other studies (Gilardoni et al., 2016; Li et al., 2021a, 2014; Xiao et al., 2022), highlighting the importance of BB emissions in atmospheric oxidation processes. This is also supported by a more recent report that intermediate VOCs emitted by BB make a considerable contribution to SOA (Li et al., 2024), reflecting the significant role of BB in the secondary formation of atmospheric organic aerosols.

To track the variation trend of fossil and non-fossil contribution to carbonaceous aerosols during the full course of haze development, the ^{14}C measurement was applied here to quantify fossil and non-fossil sources of WSOC. As presented in Table 1 and Fig. 3, the non-fossil fraction of WSOC was in the range of 18–39% (mean 26%), exhibiting fossil fuel sources were the dominant contributor to WSOC on hazy days (61–82%, 74%) (Fig. S4). Such high fossil contributions were previously observed in another megacity of Beijing during haze events in winter (~ 61%) (Zhang et al., 2017) and in spring (~ 54%) (Liu et al., 2016), and these differences in ^{14}C levels of WSOC could result from different origins and formation processes of oxygenated OC in different places and seasons. The high proportion of fossil fuels observed in this study can be attributable to extensive coal combustion for residential cooking and heating on cold days, and industrial activities and traffic emissions in the vicinity of the sampling sites could also contribute. Despite the predominance of fossil fuel sources, it is interesting to note that the contribution of non-fossils, rather than fossil fuels, increased with increasing haze pollution, suggesting non-fossil sources play a key role in the formation of heavy haze. Similarly, the non-fossil fraction of organic aerosols in northern India was found to higher during the more polluted cold period compared to the warm season (Bhattu et al., 2024). Furthermore, the highest percentages of non-fossil sources occurred in the haziest period (31 ± 6%) were coincident with the highest BB contributions during this period, which was also evidenced by the correlations between non-fossil WSOC and BB markers (e.g., syringic acid, $r = 0.68$, $p < 0.01$), indicating BB was a significant non-fossil source of WSOC and was likely

to be the important driver of heavy winter haze, despite the large amount of fossil fuel contribution at the site. This is further supported by previous reports that emphasized the contribution of aqueous-phase photochemical oxidation of BB organic gases to haze pollution (Xiao et al., 2022; Zhang et al., 2024). This aqueous-phase SOA formation could contribute more than the conventional semi-volatile SOA formation pathways, especially under polluted conditions with high relative humidity (Zhang et al., 2024). Additionally, BB-chlorine emissions could enhance oxidation capacity and further promote secondary aerosol formation (Chang et al., 2024).

3.3 Carbonaceous components

Figure 4 displays the average concentrations of carbonaceous species in $PM_{2.5}$ during three air pollution episodes. Saturated diacids (within 1.66–14.6 μg m^{-3}) were the dominant carbonaceous components of $PM_{2.5}$, followed by sugars and sugar alcohols (278–4936 ng m^{-3}) as well as anhydrosugars (79.4–801 ng m^{-3}). Higher anhydrosugar concentrations in the first episode suggest greater BB impacts during heavy haze events. In contrast, the elevated levels of sugars and sugar alcohols in the last two episodes are likely due to increased wind speeds, which enhanced the resuspension of biogenic detritus and soil microbes rich in these substances. Biogenic SOA tracers were minor species during winter haze and showed higher levels in the second episode, probably due to enhanced photooxidation under elevated temperatures and low RH. Similarly, unsaturated aliphatic diacids and aromatic acids presented the same trend as biogenic SOA. Lignin and resin acids, alternative tracers for BB, demonstrated higher concentrations in heavy haze events, as did anhydrosugars, further demonstrating the important role of BB in heavy haze. The individual organic species identified in this study are discussed below and in the Supporting Information document.

3.3.1 Biomass burning tracers (anhydrosugars and lignin/resin acids)

Levoglucosan is a specific indicator of BB and is generated from the thermal degradation of cellulose (Simoneit, 2002). The largest levoglucosan concentration was in the highest-$PM_{2.5}$ episode (average: 471 ± 122 ng m^{-3}), highlighting the remarkable contributions of BB to severe haze formation (Fig. S5). These Figures are higher than those reported in winter in Beijing

(average: 361 ng m^{-3}) (Li et al., 2018), and significantly higher than in the marine aerosols (average: 7.3 ng m^{-3}) (Kang et al., 2018a). Mannosan and galactosan, isomers of levoglucosan, are main tracers for hemicellulose pyrolysis (Simoneit, 2002). Throughout the sampling period, their concentrations were much lower than those of levoglucosan (Fig. S5 and S6). The significant correlation between mannosan and levoglucosan ($r = 0.78$, $p < 0.01$) is indicative of similar origins at this site.

The ratios of levoglucosan to potassium (L/K^+) can serve as an indicator to distinguish burning from different biomasses (Urban et al., 2012). Similar to levoglucosan, K^+ is a BB tracer as well, but there is no significant correlation between K^+ and levoglucosan in this study. This is because in urban areas airborne potassium can also be emitted from other important sources, such as meat cooking, refuse incineration, and resuspension of surface soil and fertilizers (Simoneit, 2002; Urban et al., 2012). On average, the L/K^+ ratios for three episodes were 0.51 ± 0.19, 0.20 ± 0.07, and 0.44 ± 0.33, respectively. The lower ratios observed in the second episode might be triggered by the increased wind speeds, which favor the resuspension of surface soil and fertilizers containing abundant potassium into the air (Urban et al., 2012). The enhanced chemical degradation of levoglucosan under relatively high temperatures and low RH may also contribute to lower L/K^+ ratios (Li et al., 2021b). In general, the L/K^+ values in this study (0.06–1.04) agree well with those reported for crop and wood burning (Cheng et al., 2013; Urban et al., 2012), implying a mixed biofuel combustion, as indicated by the isomeric ratios of anhydrosugars (Fig. S8).

Levoglucosan to OC (L/OC) and to EC (L/EC) ratios have long been used to assess the contribution of BB to aerosol abundance and possible degradation of levoglucosan (Mochida et al., 2010; Sullivan et al., 2008; Zhang et al., 2008). L/OC and L/EC ratios in this study are similar to those values in December in Beijing (Li et al., 2018) but higher than those in marine aerosols in winter (Zhu et al., 2015a). Relatively higher L/OC and L/EC ratios were observed in heavy haze events (Fig. S7), again proving the greater contribution of BB to heavy haze. The overall decreasing L/OC and L/EC ratios with declined $PM_{2.5}$ level might stem from reduced BB activities as well as levoglucosan degradation.

Lignin and resin acids are also reported in the smoke aerosols from BB, which can be used as BB markers as well (Simoneit, 2002). In this study, the total lignin and resin acids are found in much lower amounts than anhydrosugars (Fig. 4). A total of three lignin products (i.e., 4-hydroxybenzoic acid, vanillic acid, and syringic acid) and one resin product (dehydroabietic acid) were measured, with higher concentrations occurring in highest-$PM_{2.5}$ episode (46.5 ± 38.0 ng m^{-3}), further demonstrating significant BB influence on heavy haze. These values are comparable to those in wintertime aerosols over Beijing (47.5 ng m^{-3}) (Li et al., 2018). Specifically, syringic acid was found to be the most abundant species among lignin and resin acids during heavy haze events (~ 28.0 ng m^{-3}) while dehydroabietic acid dominated in moderate and light haze episodes (~ 14.4 and 17.0 ng m^{-3}, respectively). Dehydroabietic acid and vanillic acid are typical tracers emitted from burning of conifer (softwood fuel), while syringic acid was found enriched in hard wood smoke (Simoneit, 2002). Therefore, the relatively high levels of dehydroabietic acid and syringic acid observed in the highest-$PM_{2.5}$ episode together exhibit greater contributions of mixed wood burning on cold days, during which plentiful firewood were burned for residential cooking and heating in nearby suburbs. 4-hydroxybenzoic acid (4-HBA) is one major molecular tracer identified in the pyrolysis of non-woody vegetation including grass and crop residue, with concentrations in the range of 0.05–9.32 ng m^{-3}. A significant correlation between 4-HBA and vanillic acid was found ($r = 0.86$, $p < 0.01$), indicating similar sources such as mixed biofuel burnings.

3.3.2 Primary sugars and sugar alcohols

Primary sugars identified in this study mainly include trehalose and glucose with concentrations ranging from 86.5–3023 ng m^{-3} and 49.3–551 ng m^{-3}, respectively. Trehalose is the most abundant saccharide in soils especially in the fine mode ($PM_{2.5}$) (Jia and Fraser, 2011) and can be used as a potential tracer for resuspension of surface soil and unpaved road dust (Fu et al., 2012). This is supported by the similar change trend of trehalose and nss-Ca^{2+} in the present study, since nss-Ca^{2+} is an indicator for soil dust, particularly in winter and spring (Virkkula et al., 2006). Generally, trehalose showed higher concentrations in the second episode with an average of 1057 ± 1112 ng m^{-3}, which might be linked to the meteorological parameters like increased wind speeds relative to the other two episodes, enabling more trehalose in surface

soil to transport into the air. Glucose is also rich in biologically active soils and was proposed to be a marker for fugitive dust from cultivated land (Rogge et al., 2007). In addition, glucose is abundant in plant tissues as well, such as pollen, fruits, developing leaves, and plant detritus (Graham et al., 2003). Both glucose and trehalose presented higher levels in moderate haze events, indicating enhanced primary biogenic sources during that time due to the rising temperature and wind speeds (Zhu et al., 2015b).

Sugar alcohols detected in this study consisted of arabitol, mannitol, and glycerol with concentrations in the range of 4.59–48.2 ng m^{-3}, 0.47–24.4 ng m^{-3}, and 119–4749 ng m^{-3}, respectively. Glycerol was obviously the most abundant sugar alcohols, consistent with previous studies (Kang et al., 2018b; Li et al., 2018; Ren et al., 2020). The levels of glycerol went up when $PM_{2.5}$ concentration declined, with the highest levels present in the lowest-$PM_{2.5}$ episode (~ 2348 ng m^{-3}). Such a trend may be explained by the rising local temperature during moderate and light haze events, as lower ambient temperatures can reduce microbial activities like fungal spore release. Conversely, higher concentrations of arabitol and mannitol turned out to exist in the highest-$PM_{2.5}$ episode (> 200 μg m^{-3}), when BB greatly intensified. In addition to being emitted directly from natural sources like microbial activities and plant tissues, all these saccharides can be emitted significantly by thermal stripping during BB (Simoneit et al., 2004b). Also, BB can enhance emissions and long-range transport of some non-combusted organic compounds (Medeiros et al., 2006). It was reported that sugar alcohols were associated with airborne detritus from mature leaves and would be more prevalent during the period of leaf senescence (Graham et al., 2003; Medeiros et al., 2006), thus high levels of arabitol and mannitol can be expected in strongly BB-impacted aerosols in winter. This is further supported by the correlations between arabitol/mannitol and levoglucosan ($r = 0.39$, $p = 0.06$ and $r = 0.40$, $p = 0.06$, respectively). The above results indicate BB may have a greater effect on arabitol and mannitol than on glycerol, suggesting their main sources in the region were different.

3.3.3 Biogenic SOA tracers

The total levels of biogenic SOA tracers were in the range of 1.80–34.7 ng m^{-3}, with higher concentrations in the second episode (averaging 15.8 ng m^{-3}) as shown in Fig. 4. Isoprene-derived SOA tracers contributed more to the total biogenic SOA than monoterpene and

sesquiterpene combined (Fig. S12). The averaged ratios of isoprene to monoterpene oxidation products for three episodes were 1.16 ± 0.53, 1.44 ± 0.71, and 2.16 ± 0.94, respectively. Such values were lower than those reported in mountain aerosols, Central East China (about 4.9–6.7) (Fu et al., 2010), where large isoprene fluxes and high levels of atmospheric radicals such as OH exist.

Isoprene emitted from terrestrial vegetation is the predominant biogenic source of hydrocarbon in the atmosphere though emission of monoterpenes is quite universal among plants (Sharkey et al., 2008). Isoprene has reactive double bonds and hence can be readily oxidized by radicals (e.g., OH) as a source of tropospheric O_3 and SOA (Chameides et al., 1988; Claeys et al., 2004; Lin et al., 2013a). A total of six isoprene-SOA tracers were detected in these samples, including three C5-alkene triols, two 2-methyltetrols, and 2-methylglyceric acid (Table 1 and Fig. S10-S12). All of them showed higher levels in the second episode with average concentrations of 8.58 ± 2.52 ng m^{-3} for total isoprene-SOA, 2.20 ± 0.56 ng m^{-3} for C5-alkene triols, 3.81 ± 1.20 ng m^{-3} for 2-methyltetrols (2-MTs), 2.56 ± 0.96 ng m^{-3} for 2-methylglyceric acid (2-MGA), respectively. By comparing the temporal variations of meteorological factors and biogenic SOA concentrations (Fig. S2 and S10), it is not hard to find that the peak concentrations basically appeared under relatively high temperature and low RH conditions, in agreement with results in central China (Li et al., 2013). The similar variation patterns among isoprene SOA tracers suggest they may share common sources and be formed via similar pathways, as indicated by the significant correlations between C5-alkene triols and 2-MTs/2-MGA (r = 0.89–0.90, $p < 0.01$). 2-Methyltetrols were the dominant isoprene products (0.20–8.71 ng m^{-3}), in line with previous studies (Kang et al., 2018a; Li et al., 2018). Both 2-methyltetrols and C5-alkene triols are produced from the photooxidation of isoprene under low-NO_x (NO_x = NO+NO_2) conditions (Surratt et al., 2006, 2010) while 2-MGA is formed under high-NO_x conditions (Lin et al., 2013b; Surratt et al., 2006). The concentration ratios of C5-alkene triols to 2-methyltetrols did not exhibit significant changes except in the most polluted events (Fig. S13), which imply that their reaction processes may be different during heavy haze compared to moderate and light haze episodes. The answer may lie in the chemical structure of these two species, as C5-alkene triols have a double bond which is prone to be oxidized easily, thus the dropping ratios of C5-alkene

triols to 2-methyltetrols therefore probably reflect photochemical aging of organic aerosols over time.

Oxidation products of monoterpene include 3-hydroxyglutaricc acid (3-HGA), pinonic acid, and pinic acid. The concentrations of total monoterpene-derived SOA were in the range of 1.17–13.5 ng m^{-3}, with higher levels occurring in second episode which probably results from the enhanced photooxidation reactions due to increased temperature and declined RH. A clear correlation was found between 3-HGA and pinonic acid ($r = 0.79$, $p < 0.01$), implying similar sources and formation pathways. Pinic acid is a minor compound in monoterpene-derived SOA (0.04–1.81 ng m^{-3}), with abundances less than those of 3HGA (0.42–6.60 ng m^{-3}) and pinonic acid (0.05–6.91 ng m^{-3}) (Fig. S11). Pinic acid correlated with lignin and resin acids such as vanillic acid and 4HBA ($r = 0.69$–0.76, $p < 0.01$), suggesting BB can significantly promote its secondary formation. This is because BB is not only a significant source of air pollutants but also of oxidants (Chang et al., 2024), which enhances oxidation capacity and further promotes photochemistry and SOA formation. However, pinic acid did not exhibit the highest concentration during the heavy haze period with the greatest BB contribution. This may be due to pinic acid undergoing further reactions at high relative humidity, forming highly oxidized polar compounds through the addition of a molecule of water and the opening of the dimethylcyclobutane ring (Claeys et al., 2007).

β-caryophylinic acid is an ozonolysis or photooxidation product of β-caryophyllene (Jaoui et al., 2007), a major species of sesquiterpenes emitted from plants (Duhl et al., 2008). On the whole, there are no pronounced differences in concentrations of β-caryophylinic acid among the three episodes with the exception of a slightly higher average of 0.29 ng m^{-3} in the lowest-$PM_{2.5}$ event (< 100 μg m^{-3}).

3.3.4 Aromatic acids

Three aromatic acids containing two phthalic acids (phthalic acid and isophthalic acid) and benzoic acid were determined in these aerosols. Relatively higher total abundances of aromatic acids occurred in high-$PM_{2.5}$ episodes (> 100 μg m^{-3}) with a concentration range of 8.3–45.1 ng m^{-3}. Phthalic acid (Ph) and isophthalic acid (iPh) were the major aromatic acids, with

concentrations in the range of 1.45–13.0 ng m^{-3} and 0.98–21.2 ng m^{-3}, respectively. The secondary photochemical reactions of polycyclic aromatic hydrocarbons (PAHs) such as naphthalene are possibly the main sources of Ph, which has been proposed as a naphthalene-derived SOA tracer (Fine et al., 2004; Ren et al., 2020). Vehicle exhausts are important sources of naphthalene in urban atmosphere, and therefore transportation emissions were likely to be responsible for the Ph over this site. By comparison, benzoic acid was a minor species in aromatic acids (0.47–11.4 ng m^{-3}). It can be directly emitted from vehicle exhaust and secondarily produced through photochemical reactions of aromatic hydrocarbons from traffic emissions such as toluene (Ho et al., 2015; Li et al., 2022; Rogge et al., 1993; Suh et al., 2003). The relationships among Ph, iPh, and benzoic acid ($r = 0.64–0.79$, $p < 0.01$) suggest they share common sources, such as fossil fuels.

3.3.5 Hydroxy-/polyacids

Polyacids are reported to be secondary photooxidation products of atmospheric organic precursors (Fu et al., 2008; Kawamura and Sakaguchi, 1999). A total of three hydroxy-/polyacids were measured, including glyceric acid, malic acid, and tartaric acid. The slightly higher content of hydroxy-/polyacids in second episode may be due to enhanced photooxidation reactions under increased temperature and low RH. Malic acid (0.77–6.60 ng m^{-3}) is the major compound in hydroxy carboxylic acids, followed by glyceric acid (0.22–6.56 ng m^{-3}), while tartaric acid is relatively minor. The above result is consistent with an early report over the polluted East Asia/Pacific region (Simoneit et al., 2004a). In current study, glyceric acid was significantly correlated with tartaric acid ($r = 0.81$, $p < 0.01$), implying similar sources and/or formation pathways. Moreover, glyceric and tartaric acid were found to be significantly correlated with isoprene ($r = 0.71–0.93$, $p < 0.01$) and monoterpene ($r = 0.65–0.77$, $p < 0.01$) SOA tracers (e.g., 2-methyltetrols, C5-alkene triols, pinic, and pinonic) while malic acid was positively correlated with glucose ($r = 0.65$, $p < 0.01$). These significant relationships suggest that hydroxy-acids may be secondary oxidation products of biogenic VOCs and sugars (Simoneit et al., 2004a). There were also pronounced correlations between glyceric acid and aromatic acids such as iPh and benzoic acid ($r = 0.63–0.71$, $p < 0.01$), implying that they may undergo similar atmospheric processing pathways. In addition, glyceric and tartaric acids were

significantly correlated with 4HBA and vanillic acid (r = 0.58–0.81, $p < 0.01$), indicating BB contribute to the secondary production of hydroxy-acids.

3.3.6 Dicarboxylic acids

Dicarboxylic acids are predominantly present as air particles rather than in the gas phase due to their low vapor pressures (Limbeck et al., 2001; Saxena and Hildemann, 1996). They contain two carboxyl groups and are the major constituents of water-soluble organics in aerosols (Saxena and Hildemann, 1996), as proved by the significant correlation between WSOC and dicarboxylic acids in this study (r = 0.74–0.87, $p < 0.01$). In addition to being directly released into the air from incomplete combustion of fossil fuels, meat cooking, and biomass burning, they can be also formed by secondary photochemical reactions (Mochida et al., 2003). For instance, isoprene and unsaturated fatty acids are proposed to be sources of dicarboxylic acids in the open ocean (Bikkina et al., 2014). Totally, four saturated dicarboxylic acids (i.e., oxalic, malonic, succinic, and glutaric acid) and two unsaturated dicarboxylic acids (maleic and fumaric acid) were included here. The levels of unsaturated-dicarboxylic acids (2.48–69.5 ng m^{-3}) were far less than those of saturated diacids (1.66–14.6 μg m^{-3}). Similar to biogenic SOA, dicarboxylic acids showed higher concentrations in the episode with relatively high temperature and low RH (Fig. 4), which are beneficial for the photochemical oxidation of organic precursors.

Malonic acid (C3, 1.48–14.3 μg m^{-3}) was the most abundant species among measured dicarboxylic acids, followed by oxalic acid (C2, 0.09–0.74 μg m^{-3}). C2 and C4 (succinic acid) levels are comparable to those reported in $PM_{2.5}$ aerosols from megacities such as Beijing (Ho et al., 2010) and Guangzhou (Liu et al., 2021). It was deduced that C2 and C3 diacids are likely produced by the oxidation of C4 and other longer chain diacids, whereas those longer-chain diacids (C5–C10) are formed by oxidation of unsaturated fatty acids (Kawamura and Gagosian, 1987; Kawamura and Sakaguchi, 1999). This conclusion is supported by the significant correlations between C2 and C4 (r = 0.86, $p < 0.01$), C2 and C5 (glutaric acid) (r = 0.77, $p < 0.01$) and C4 and C5 (r = 0.60, $p < 0.01$) in the present study. In comparison with other diacids identified in this study, the relatively higher levels of C2 and C3 may partially result from considerable photodegradation of C4 and C5 in haze events, implying these urban aerosols may have undergone great aging processes. The ratio of C3 to C4 is a useful indicator for elevated

photochemical production of dicarboxylic acids in the atmosphere, as C4 is a precursor of C3 formation (Kawamura and Ikushima, 1993). In this study, C3 dicarboxylic acid was far more abundant than C4 indicating strong photochemical processes, as also suggested by the high WSOC/OC ratios mentioned earlier. Such findings mean secondary formation is an important pathway of dicarboxylic acids on hazy days in urban Nanjing, apart from primary emissions. It should be noted that C2 and C5 both correlated well with levoglucosan ($r = 0.66–0.69$, $p < 0.01$), indicating BB is an alternative source of these diacids and/or can facilitate their oxidation reaction (Kawamura and Bikkina, 2016). Chlorine emissions from BB were found to increase oxidant levels, such as O_3 and OH radicals, largely impacting atmospheric chemistry and oxidation process (Chang et al., 2024).

3.4 Contributions of primary and secondary sources to OC

To evaluate the contribution of primary (e.g., BB, fungal spores, and plant debris) and secondary sources (e.g., oxidation reactions of PAHs and biogenic VOCs including isoprene, monoterpene, and sesquiterpene) to OC in $PM_{2.5}$, tracer-based methods were applied here. Details about specific calculation methods and relevant conversion factors can be found in our previous work and other reports (Bauer et al., 2008a; Gelencsér et al., 2007; Holden et al., 2011; Kang et al., 2018a; Kleindienst et al., 2007, 2012; Puxbaum and Tenze-Kunit, 2003).

Compared with other primary and secondary sources, BB made an absolutely predominant contribution to aerosol OC throughout the whole sampling period, both in concentration and in proportion (0.72–8.86 μg m^{-3} and 8.29–26.5%). The greatest impact of BB was observed during heavy haze events (mean: 5.79 ± 1.50 μg m^{-3}, 16.3 ± 3.39%). This could be attributed to the increased domestic wood/crop combustion for heating and cooking, along with biomass burning in the surrounding area, driven by low temperatures and high relative humidity during this period (Figs. S1-S2). BB-chlorine emissions have been shown to elevate O_3 and OH radical levels, significantly impacting oxidation processes (Chang et al., 2024). In addition, soluble organic gases from BB can dissolve in aerosol/cloud liquid water and subsequently react with aqueous phase oxidants to form SOA, with these reactions increasing with increasing RH (Zhang et al., 2024). Considering the potential atmospheric degradation of levoglucosan, the contribution of BB might be somewhat underestimated and thus the actual BB fraction is likely

555 larger, highlighting the crucial role of BB in haze formation. A higher relative contribution of
556 BB to organic aerosols during the colder period, characterized by elevated $PM_{2.5}$ concentrations,
557 was also recently reported in northern India (Bhattu et al., 2024). Relatively high concentration
558 of fungal-spores-derived OC occurred in the highest-$PM_{2.5}$ episode (0.44 ± 0.14 μg m^{-3}) when
559 BB impacts were significant (Fig. S15), consistent with an earlier study that observed elevated
560 fungal spore tracers on BB-affected days (Yang et al., 2012). This suggests that BB could raise
561 emissions from other sources, such as fungal spores, further exacerbating air pollution.
562 Nonetheless, percentages of fungal spores to OC were on the decline with increasing $PM_{2.5}$
563 levels with higher fractions displaying in light haze episode (2.38 ± 2.26%), during which the
564 contribution of BB to OC remained high (15.9 ± 7.01%). By comparison, concentrations and
565 contributions of OC from plant debris were higher in the second episode (0.45 ± 0.21 μg m^{-3},
566 1.99 ± 1.02%), probably on account of increased resuspension of surface soils and road dust
567 resulting from elevated wind speeds and temperatures (Simoneit et al., 2004b). The total
568 abundance of primary OC derived from BB, fungal spores and plant debris ranges from 1.23 to
569 9.65 μg m^{-3} making up 11.3–31.3% of OC, with higher concentrations in the most polluted
570 episode (average: 6.52 ± 1.62 μg m^{-3}, 18.4 ± 3.62%). It is noteworthy that despite lower
571 concentrations of total primary OC in light haze episode ($PM_{2.5}$ < 100 μg m^{-3}), the contribution
572 of primary OC to aerosol OC was comparable to and even bigger (19.9 ± 8.31%) than those in
573 heavy and moderate episodes.

574 By comparison, secondary sources (i.e., isoprene, monoterpene, sesquiterpene, and naphthalene)
575 contributed less than primary sources, accounting for only 0.38–3.56% of OC in $PM_{2.5}$, which
576 probably arose from reduced photolysis during winter due to less intense sunlight. Overall, SOC
577 showed high levels (0.36 ± 0.07 μg m^{-3}) and high contributions (1.53 ± 0.37%) during periods
578 of high temperatures and low RH, because such weather conditions promote increased
579 photochemical reactions and the production of SOC in the atmosphere. It is notable that
580 naphthalene-derived SOC was the main secondary source of OC, both in concentration (0.04–
581 0.34 μg m^{-3}) and in proportion (0.27–2.46%) (Table 2), followed by biogenic isoprene-derived
582 SOC (0.003–0.09 μg m^{-3}, 0.01–0.60%), indicating anthropogenic VOCs make a dominate
583 contribution to SOC in these urban aerosols. Moreover, the total concentrations and fractional

584 contributions of these biogenic SOCs (0.01–0.16 μg m^{-3}, 0.05–1.10%) were lower than those
585 from anthropogenic sources, probably due to significantly reduced biogenic VOC emissions
586 and largely increased fossil fuel combustion during cold winter periods. The abundance and
587 percentage of total primary and secondary OC were 1.54–9.98 μg m^{-3} and 11.9–32.2%,
588 respectively, based on the detected tracers in this study. Such values are comparable to those
589 reported in winter aerosol in Beijing (6.18–38.3%) (Li et al., 2018).

590 **4. Conclusions**

591 Molecular distributions and high temporal variations of primary and secondary components in
592 $PM_{2.5}$ during winter hazy episodes in urban Nanjing were comprehensively characterized
593 through intensive sampling. Our results revealed that OM dominated the total $PM_{2.5}$, followed
594 by NO_3^-. ^{14}C analysis showed that while fossil fuel sources primarily contributed to WSOC,
595 non-fossil sources, notably BB, became more significant as $PM_{2.5}$ pollution intensified. BB
596 made a dominant contribution to OC, particularly during severe haze events, likely due to
597 aqueous SOA formation from BB-derived organic gases. Other non-fossil sources like fungal
598 spores were also elevated by BB, whereas plant debris contributions were higher on lighter hazy
599 days with higher wind speeds and temperatures. Overall, these findings highlight the significant
600 role of BB in winter haze over Nanjing and underscore the need for further research into the
601 molecular-level identification of gaseous species from BB emissions and their role in secondary
602 aerosol formation. Additionally, although meteorological parameters have an important
603 influence on the development of heavy haze, accurately quantifying their contribution remains
604 a challenge for future research.
605

606 **Data availability**. The dataset for this paper is available upon request from the corresponding
607 author (zhangyanlin@nuist.edu.cn).

608 **Supplement.** Information on Chloride, unsaturated diacids, monocarboxylic acids,
609 Methylglyoxal, Methanesulfonic acid (MSA) in $PM_{2.5}$ were investigated here. HYSPLIT back
610 trajectories initiated over Nanjing (Fig. S1). Time series of meteorological parameters (Fig. S2).
611 Relationship between EC and OC in $PM_{2.5}$ (Fig. S3). Temporal variations of fossil and non-

fossil contribution to WSOC (Fig. S4). Temporal variations of biomass burning tracers along with the average concentrations of anhydrosugars and lignin and resin products detected in three episodes (Fig. S5-S6). Temporal variations of ratios of L/M, L/OC, and L/EC, and the average ratios during three episodes (Fig. S7). Comparison of L/M and M/G ratios from literature values and ambient aerosols in this study (Fig. S8). Temporal variations of sugars, sugar alcohols, and biogenic SOA tracers (Fig. S9-S10). Average concentrations of biogenic SOA tracers detected in three episodes (Fig. S11-S12). Temporal variations in the concentration ratios of isoprene oxidation products (Fig. S13). Temporal variations in the biogenic SOC derived from isoprene, monoterpene, and sesquiterpene (Fig. S14). Temporal variations in biomass burning-derived OC, fungal spores-derived OC, and plant debris-derived OC (Fig. S15).

Author contributions. YLZ designed the research. MYB collected aerosol samples. MYB and WHS performed the laboratory analyses. The paper was written by MJK with editing from all co-authors.

Competing interests. The authors declare that they have no conflict of interest.

Acknowledgments

This work was supported by the National Natural Science Foundation of China (No. 42192512, 42273087, and 42307142).

References

Alexeeff, S. E., Deosaransingh, K., Van Den Eeden, S., Schwartz, J., Liao, N. S., and Sidney, S.: Association of Long-term Exposure to Particulate Air Pollution With Cardiovascular Events in California, JAMA Network Open, 6, e230561, https://doi.org/10.1001/jamanetworkopen.2023.0561, 2023.

Andreae, M. O. and Merlet, P.: Emission of trace gases and aerosols from biomass burning, Global Biogeochemical Cycles, 15, 955–966, https://doi.org/10.1029/2000GB001382, 2001.

Anon: Biomass burning — a review of organic tracers for smoke from incomplete combustion, Applied Geochemistry, 17, 129–162, https://doi.org/10.1016/S0883-2927(01)00061-0, 2002.

Bao, M., Zhang, Y.-L., Cao, F., Lin, Y.-C., Hong, Y., Fan, M., Zhang, Y., Yang, X., and Xie, F.: Light absorption and source apportionment of water soluble humic-like substances (HULIS) in PM2.5 at Nanjing, China, Environmental Research, 206, 112554, https://doi.org/10.1016/j.envres.2021.112554, 2022.

Bao, M., Zhang, Y.-L., Cao, F., Hong, Y., Lin, Y.-C., Yu, M., Jiang, H., Cheng, Z., Xu, R., and Yang, X.: Impact of fossil and non-fossil fuel sources on the molecular compositions of water-soluble humic-like substances in $PM_{2.5}$ at a suburban site of Yangtze River Delta, China, Atmospheric Chemistry and Physics, 23, 8305–8324, https://doi.org/10.5194/acp-23-8305-2023, 2023.

Bauer, H., Claeys, M., Vermeylen, R., Schueller, E., Weinke, G., Berger, A., and Puxbaum, H.: Arabitol and mannitol as tracers for the quantification of airborne fungal spores, Atmospheric Environment, 42, 588–593, https://doi.org/10.1016/j.atmosenv.2007.10.013, 2008a.

Bauer, H., Schueller, E., Weinke, G., Berger, A., Hitzenberger, R., Marr, I. L., and Puxbaum, H.: Significant contributions of fungal spores to the organic carbon and to the aerosol mass balance of the urban atmospheric aerosol, Atmospheric Environment, 42, 5542–5549, https://doi.org/10.1016/j.atmosenv.2008.03.019, 2008b.

Bhattu, D., Tripathi, S. N., Bhowmik, H. S., Moschos, V., Lee, C. P., Rauber, M., Salazar, G., Abbaszade, G., Cui, T., Slowik, J. G., Vats, P., Mishra, S., Lalchandani, V., Satish, R., Rai, P., Casotto, R., Tobler, A., Kumar, V., Hao, Y., Qi, L., Khare, P., Manousakas, M. I., Wang, Q., Han, Y., Tian, J., Darfeuil, S., Minguillon, M. C., Hueglin, C., Conil, S., Rastogi, N., Srivastava, A. K., Ganguly, D., Bjelic, S., Canonaco, F., Schnelle-Kreis, J., Dominutti, P. A., Jaffrezo, J.-L., Szidat, S., Chen, Y., Cao, J., Baltensperger, U., Uzu, G., Daellenbach, K. R., El Haddad, I., and Prévôt, A. S. H.: Local incomplete combustion emissions define the PM2.5 oxidative potential in Northern India, Nat Commun, 15, 3517, https://doi.org/10.1038/s41467-024-47785-5, 2024.

Bikkina, S., Kawamura, K., Miyazaki, Y., and Fu, P.: High abundances of oxalic, azelaic, and glyoxylic acids and methylglyoxal in the open ocean with high biological activity: Implication for secondary OA formation from isoprene, Geophysical Research Letters, 41, 3649–3657, https://doi.org/10.1002/2014GL059913, 2014.

Boreddy, S. K. R., Haque, M. M., and Kawamura, K.: Long-term (2001–2012) trends of carbonaceous aerosols from a remote island in the western North Pacific: an outflow region of Asian pollutants, Atmospheric Chemistry and Physics, 18, 1291–1306, https://doi.org/10.5194/acp-18-1291-2018, 2018.

Chameides, W. L., Lindsay, R. W., Richardson, J., and Kiang, C. S.: The Role of Biogenic Hydrocarbons in Urban Photochemical Smog: Atlanta as a Case Study, Science, 241, 1473–1475, https://doi.org/10.1126/science.3420404, 1988.

Chang, D., Li, Q., Wang, Z., Dai, J., Fu, X., Guo, J., Zhu, L., Pu, D., Cuevas, C. A., Fernandez, R. P., Wang, W., Ge, M., Fung, J. C. H., Lau, A. K. H., Granier, C., Brasseur, G., Pozzer, A., Saiz-Lopez, A., Song, Y., and Wang, T.: Significant chlorine emissions from biomass burning affect the long-term atmospheric chemistry in Asia, National Science Review, nwae285, https://doi.org/10.1093/nsr/nwae285, 2024.

Chang, X., Wang, S., Zhao, B., Xing, J., Liu, X., Wei, L., Song, Y., Wu, W., Cai, S., Zheng, H., Ding, D., and Zheng, M.: Contributions of inter-city and regional transport to PM2.5 concentrations in the Beijing-Tianjin-Hebei region and its implications on regional joint air pollution control, Science of The Total Environment, 660, 1191–1200, https://doi.org/10.1016/j.scitotenv.2018.12.474, 2019.

687 Chen, D., Liu, X., Lang, J., Zhou, Y., Wei, L., Wang, X., and Guo, X.: Estimating the
688 contribution of regional transport to PM2.5 air pollution in a rural area on the North China
689 Plain, Science of The Total Environment, 583, 280–291,
690 https://doi.org/10.1016/j.scitotenv.2017.01.066, 2017a.
691 Chen, J., Li, C., Ristovski, Z., Milic, A., Gu, Y., Islam, M. S., Wang, S., Hao, J., Zhang, H., He,
692 C., Guo, H., Fu, H., Miljevic, B., Morawska, L., Thai, P., Lam, Y. F., Pereira, G., Ding, A.,
693 Huang, X., and Dumka, U. C.: A review of biomass burning: Emissions and impacts on air
694 quality, health and climate in China, Science of The Total Environment, 579, 1000–1034,
695 https://doi.org/10.1016/j.scitotenv.2016.11.025, 2017b.
696 Chen, R., Jiang, Y., Hu, J., Chen, H., Li, H., Meng, X., Ji, J. S., Gao, Y., Wang, W., Liu, C.,
697 Fang, W., Yan, H., Chen, J., Wang, W., Xiang, D., Su, X., Yu, B., Wang, Y., Xu, Y., Wang,
698 L., Li, C., Chen, Y., Bell, M. L., Cohen, A. J., Ge, J., Huo, Y., and Kan, H.: Hourly Air
699 Pollutants and Acute Coronary Syndrome Onset in 1.29 Million Patients, Circulation, 145,
700 1749–1760, https://doi.org/10.1161/CIRCULATIONAHA.121.057179, 2022.
701 Cheng, Y., Engling, G., He, K.-B., Duan, F.-K., Ma, Y.-L., Du, Z.-Y., Liu, J.-M., Zheng, M., and
702 Weber, R. J.: Biomass burning contribution to Beijing aerosol, Atmospheric Chemistry and
703 Physics, 13, 7765–7781, https://doi.org/10.5194/acp-13-7765-2013, 2013.
704 Cheng, Y., Zheng, G., Wei, C., Mu, Q., Zheng, B., Wang, Z., Gao, M., Zhang, Q., He, K.,
705 Carmichael, G., Pöschl, U., and Su, H.: Reactive nitrogen chemistry in aerosol water as a
706 source of sulfate during haze events in China, Science Advances, 2, e1601530,
707 https://doi.org/10.1126/sciadv.1601530, 2016.
708 Claeys, M., Graham, B., Vas, G., Wang, W., Vermeylen, R., Pashynska, V., Cafmeyer, J., Guyon,
709 P., Andreae, M. O., Artaxo, P., and Maenhaut, W.: Formation of Secondary Organic
710 Aerosols Through Photooxidation of Isoprene, Science, 303, 1173–1176,
711 https://doi.org/10.1126/science.1092805, 2004.
712 Claeys, M., Szmigielski, R., Kourtchev, I., Van der Veken, P., Vermeylen, R., Maenhaut, W.,
713 Jaoui, M., Kleindienst, T. E., Lewandowski, M., Offenberg, J. H., and Edney, E. O.:
714 Hydroxydicarboxylic Acids: Markers for Secondary Organic Aerosol from the
715 Photooxidation of α-Pinene, Environ. Sci. Technol., 41, 1628–1634,
716 https://doi.org/10.1021/es0620181, 2007.
717 Ding, X., Zhang, Y.-Q., He, Q.-F., Yu, Q.-Q., Wang, J.-Q., Shen, R.-Q., Song, W., Wang, Y.-S.,
718 and Wang, X.-M.: Significant Increase of Aromatics-Derived Secondary Organic Aerosol
719 during Fall to Winter in China, Environ. Sci. Technol., 51, 7432–7441,
720 https://doi.org/10.1021/acs.est.6b06408, 2017.
721 Duhl, T. R., Helmig, D., and Guenther, A.: Sesquiterpene emissions from vegetation: a review,
722 Biogeosciences, 5, 761–777, https://doi.org/10.5194/bg-5-761-2008, 2008.
723 Elias, V. O., Simoneit, B. R. T., Cordeiro, R. C., and Turcq, B.: Evaluating levoglucosan as an
724 indicator of biomass burning in Carajás, amazônia: a comparison to the charcoal record2,
725 Geochimica et Cosmochimica Acta, 65, 267–272, https://doi.org/10.1016/S0016-
726 7037(00)00522-6, 2001.
727 Fan, M.-Y., Zhang, Y.-L., Lin, Y.-C., Cao, F., Zhao, Z.-Y., Sun, Y., Qiu, Y., Fu, P., and Wang, Y.:
728 Changes of Emission Sources to Nitrate Aerosols in Beijing After the Clean Air Actions:
729 Evidence From Dual Isotope Compositions, Journal of Geophysical Research:
730 Atmospheres, 125, e2019JD031998, https://doi.org/10.1029/2019JD031998, 2020.

Fan, M.-Y., Zhang, W., Zhang, Y.-L., Li, J., Fang, H., Cao, F., Yan, M., Hong, Y., Guo, H., and Michalski, G.: Formation Mechanisms and Source Apportionments of Nitrate Aerosols in a Megacity of Eastern China Based On Multiple Isotope Observations, Journal of Geophysical Research: Atmospheres, 128, e2022JD038129, https://doi.org/10.1029/2022JD038129, 2023.

Fine, P. M., Chakrabarti, B., Krudysz, M., Schauer, J. J., and Sioutas, C.: Diurnal Variations of Individual Organic Compound Constituents of Ultrafine and Accumulation Mode Particulate Matter in the Los Angeles Basin, Environ. Sci. Technol., 38, 1296–1304, https://doi.org/10.1021/es0348389, 2004.

Fu, P., Kawamura, K., Okuzawa, K., Aggarwal, S. G., Wang, G., Kanaya, Y., and Wang, Z.: Organic molecular compositions and temporal variations of summertime mountain aerosols over Mt. Tai, North China Plain, Journal of Geophysical Research: Atmospheres, 113, https://doi.org/10.1029/2008JD009900, 2008.

Fu, P., Kawamura, K., Kanaya, Y., and Wang, Z.: Contributions of biogenic volatile organic compounds to the formation of secondary organic aerosols over Mt. Tai, Central East China, Atmospheric Environment, 44, 4817–4826, https://doi.org/10.1016/j.atmosenv.2010.08.040, 2010.

Fu, P., Kawamura, K., Kobayashi, M., and Simoneit, B. R. T.: Seasonal variations of sugars in atmospheric particulate matter from Gosan, Jeju Island: Significant contributions of airborne pollen and Asian dust in spring, Atmospheric Environment, 55, 234–239, https://doi.org/10.1016/j.atmosenv.2012.02.061, 2012.

Fu, P., Kawamura, K., Chen, J., and Miyazaki, Y.: Secondary production of organic aerosols from biogenic VOCs over Mt. Fuji, Japan, Environmental science & technology, 48, 8491–8497, 2014.

Fu, P., Zhuang, G., Sun, Y., Wang, Q., Chen, J., Ren, L., Yang, F., Wang, Z., Pan, X., Li, X., and Kawamura, K.: Molecular markers of biomass burning, fungal spores and biogenic SOA in the Taklimakan desert aerosols, Atmospheric Environment, 130, 64–73, https://doi.org/10.1016/j.atmosenv.2015.10.087, 2016.

Gelencsér, A., May, B., Simpson, D., Sánchez-Ochoa, A., Kasper-Giebl, A., Puxbaum, H., Caseiro, A., Pio, C., and Legrand, M.: Source apportionment of PM2.5 organic aerosol over Europe: Primary/secondary, natural/anthropogenic, and fossil/biogenic origin, Journal of Geophysical Research: Atmospheres, 112, https://doi.org/10.1029/2006JD008094, 2007.

Gilardoni, S., Massoli, P., Paglione, M., Giulianelli, L., Carbone, C., Rinaldi, M., Decesari, S., Sandrini, S., Costabile, F., Gobbi, G. P., Pietrogrande, M. C., Visentin, M., Scotto, F., Fuzzi, S., and Facchini, M. C.: Direct observation of aqueous secondary organic aerosol from biomass-burning emissions, Proceedings of the National Academy of Sciences, 113, 10013–10018, https://doi.org/10.1073/pnas.1602212113, 2016.

Graham, B., Guyon, P., Taylor, P. E., Artaxo, P., Maenhaut, W., Glovsky, M. M., Flagan, R. C., and Andreae, M. O.: Organic compounds present in the natural Amazonian aerosol: Characterization by gas chromatography–mass spectrometry, Journal of Geophysical Research: Atmospheres, 108, https://doi.org/10.1029/2003JD003990, 2003.

Griffin, R. J., Cocker III, D. R., Seinfeld, J. H., and Dabdub, D.: Estimate of global atmospheric organic aerosol from oxidation of biogenic hydrocarbons, Geophysical Research Letters, 26, 2721–2724, https://doi.org/10.1029/1999GL900476, 1999.

Guenther, A., Karl, T., Harley, P., Wiedinmyer, C., Palmer, P. I., and Geron, C.: Estimates of global terrestrial isoprene emissions using MEGAN (Model of Emissions of Gases and Aerosols from Nature), Atmospheric Chemistry and Physics, 6, 3181–3210, https://doi.org/10.5194/acp-6-3181-2006, 2006.

Hallquist, M., Wenger, J. C., Baltensperger, U., Rudich, Y., Simpson, D., Claeys, M., Dommen, J., Donahue, N. M., George, C., Goldstein, A. H., Hamilton, J. F., Herrmann, H., Hoffmann, T., Iinuma, Y., Jang, M., Jenkin, M. E., Jimenez, J. L., Kiendler-Scharr, A., Maenhaut, W., McFiggans, G., Mentel, T. F., Monod, A., Prévôt, A. S. H., Seinfeld, J. H., Surratt, J. D., Szmigielski, R., and Wildt, J.: The formation, properties and impact of secondary organic aerosol: current and emerging issues, Atmospheric Chemistry and Physics, 9, 5155–5236, https://doi.org/10.5194/acp-9-5155-2009, 2009.

Ho, K. F., Lee, S. C., Ho, S. S. H., Kawamura, K., Tachibana, E., Cheng, Y., and Zhu, T.: Dicarboxylic acids, ketocarboxylic acids, α-dicarbonyls, fatty acids, and benzoic acid in urban aerosols collected during the 2006 Campaign of Air Quality Research in Beijing (CAREBeijing-2006), Journal of Geophysical Research: Atmospheres, 115, https://doi.org/10.1029/2009JD013304, 2010.

Ho, K. F., Huang, R.-J., Kawamura, K., Tachibana, E., Lee, S. C., Ho, S. S. H., Zhu, T., and Tian, L.: Dicarboxylic acids, ketocarboxylic acids, α-dicarbonyls, fatty acids and benzoic acid in $PM_{2.5}$ aerosol collected during CAREBeijing-2007: an effect of traffic restriction on air quality, Atmospheric Chemistry and Physics, 15, 3111–3123, https://doi.org/10.5194/acp-15-3111-2015, 2015.

Holden, A. S., Sullivan, A. P., Munchak, L. A., Kreidenweis, S. M., Schichtel, B. A., Malm, W. C., and Collett, J. L.: Determining contributions of biomass burning and other sources to fine particle contemporary carbon in the western United States, Atmospheric Environment, 45, 1986–1993, https://doi.org/10.1016/j.atmosenv.2011.01.021, 2011.

Huang, R.-J., Zhang, Y., Bozzetti, C., Ho, K.-F., Cao, J.-J., Han, Y., Daellenbach, K. R., Slowik, J. G., Platt, S. M., Canonaco, F., Zotter, P., Wolf, R., Pieber, S. M., Bruns, E. A., Crippa, M., Ciarelli, G., Piazzalunga, A., Schwikowski, M., Abbaszade, G., Schnelle-Kreis, J., Zimmermann, R., An, Z., Szidat, S., Baltensperger, U., Haddad, I. E., and Prévôt, A. S. H.: High secondary aerosol contribution to particulate pollution during haze events in China, Nature, 514, 218–222, https://doi.org/10.1038/nature13774, 2014.

Huang, X., Ding, A., Wang, Z., Ding, K., Gao, J., Chai, F., and Fu, C.: Amplified transboundary transport of haze by aerosol–boundary layer interaction in China, Nat. Geosci., 13, 428–434, https://doi.org/10.1038/s41561-020-0583-4, 2020a.

Huang, X., Ding, A., Gao, J., Zheng, B., Zhou, D., Qi, X., Tang, R., Wang, J., Ren, C., Nie, W., Chi, X., Xu, Z., Chen, L., Li, Y., Che, F., Pang, N., Wang, H., Tong, D., Qin, W., Cheng, W., Liu, W., Fu, Q., Liu, B., Chai, F., Davis, S. J., Zhang, Q., and He, K.: Enhanced secondary pollution offset reduction of primary emissions during COVID-19 lockdown in China, National Science Review, https://doi.org/10.1093/nsr/nwaa137, 2020b.

Jaoui, M., Lewandowski, M., Kleindienst, T. E., Offenberg, J. H., and Edney, E. O.: β-caryophyllinic acid: An atmospheric tracer for β-caryophyllene secondary organic aerosol, Geophysical Research Letters, 34, https://doi.org/10.1029/2006GL028827, 2007.

Ji, D., Gao, W., Maenhaut, W., He, J., Wang, Z., Li, J., Du, W., Wang, L., Sun, Y., Xin, J., Hu, B., and Wang, Y.: Impact of air pollution control measures and regional transport on carbonaceous aerosols in fine particulate matter in urban Beijing, China: insights gained from long-term measurement, Atmospheric Chemistry and Physics, 19, 8569–8590, https://doi.org/10.5194/acp-19-8569-2019, 2019.

Jia, Y. and Fraser, M.: Characterization of Saccharides in Size-fractionated Ambient Particulate Matter and Aerosol Sources: The Contribution of Primary Biological Aerosol Particles (PBAPs) and Soil to Ambient Particulate Matter, Environ. Sci. Technol., 45, 930–936, https://doi.org/10.1021/es103104e, 2011.

Jimenez, J. L., Canagaratna, M. R., Donahue, N. M., Prevot, A. S. H., Zhang, Q., Kroll, J. H., DeCarlo, P. F., Allan, J. D., Coe, H., Ng, N. L., Aiken, A. C., Docherty, K. S., Ulbrich, I. M., Grieshop, A. P., Robinson, A. L., Duplissy, J., Smith, J. D., Wilson, K. R., Lanz, V. A., Hueglin, C., Sun, Y. L., Tian, J., Laaksonen, A., Raatikainen, T., Rautiainen, J., Vaattovaara, P., Ehn, M., Kulmala, M., Tomlinson, J. M., Collins, D. R., Cubison, M. J., E., Dunlea, J., Huffman, J. A., Onasch, T. B., Alfarra, M. R., Williams, P. I., Bower, K., Kondo, Y., Schneider, J., Drewnick, F., Borrmann, S., Weimer, S., Demerjian, K., Salcedo, D., Cottrell, L., Griffin, R., Takami, A., Miyoshi, T., Hatakeyama, S., Shimono, A., Sun, J. Y., Zhang, Y. M., Dzepina, K., Kimmel, J. R., Sueper, D., Jayne, J. T., Herndon, S. C., Trimborn, A. M., Williams, L. R., Wood, E. C., Middlebrook, A. M., Kolb, C. E., Baltensperger, U., and Worsnop, D. R.: Evolution of Organic Aerosols in the Atmosphere, Science, 326, 1525–1529, https://doi.org/10.1126/science.1180353, 2009.

Kanakidou, M., Seinfeld, J. H., Pandis, S. N., Barnes, I., Dentener, F. J., Facchini, M. C., Dingenen, R. V., Ervens, B., Nenes, A., Nielsen, C. J., Swietlicki, E., Putaud, J. P., Balkanski, Y., Fuzzi, S., Horth, J., Moortgat, G. K., Winterhalter, R., Myhre, C. E. L., Tsigaridis, K., Vignati, E., Stephanou, E. G., and Wilson, J.: Organic aerosol and global climate modelling: a review, Atmospheric Chemistry and Physics, 5, 1053–1123, https://doi.org/10.5194/acp-5-1053-2005, 2005.

Kang, M., Fu, P., Aggarwal, S. G., Kumar, S., Zhao, Y., Sun, Y., and Wang, Z.: Size distributions of n-alkanes, fatty acids and fatty alcohols in springtime aerosols from New Delhi, India, Environmental Pollution, 219, 957–966, https://doi.org/10.1016/j.envpol.2016.09.077, 2016.

Kang, M., Fu, P., Kawamura, K., Yang, F., Zhang, H., Zang, Z., Ren, H., Ren, L., Zhao, Y., Sun, Y., and Wang, Z.: Characterization of biogenic primary and secondary organic aerosols in the marine atmosphere over the East China Sea, Atmospheric Chemistry and Physics, 18, 13947–13967, https://doi.org/10.5194/acp-18-13947-2018, 2018a.

Kang, M., Ren, L., Ren, H., Zhao, Y., Kawamura, K., Zhang, H., Wei, L., Sun, Y., Wang, Z., and Fu, P.: Primary biogenic and anthropogenic sources of organic aerosols in Beijing, China: Insights from saccharides and n-alkanes, Environmental Pollution, 243, 1579–1587, https://doi.org/10.1016/j.envpol.2018.09.118, 2018b.

Kang, M., Guo, H., Wang, P., Fu, P., Ying, Q., Liu, H., Zhao, Y., and Zhang, H.: Characterization and source apportionment of marine aerosols over the East China Sea, Science of The Total Environment, 651, 2679–2688, https://doi.org/10.1016/j.scitotenv.2018.10.174, 2019.

Kang, M., Zhang, J., Zhang, H., and Ying, Q.: On the Relevancy of Observed Ozone Increase during COVID-19 Lockdown to Summertime Ozone and PM2.5 Control Policies in China, Environ. Sci. Technol. Lett., 8, 289–294, https://doi.org/10.1021/acs.estlett.1c00036, 2021.

Kaufman, Y. J., Tanré, D., and Boucher, O.: A satellite view of aerosols in the climate system, Nature, 419, 215–223, https://doi.org/10.1038/nature01091, 2002.

Kawamura, K. and Bikkina, S.: A review of dicarboxylic acids and related compounds in atmospheric aerosols: Molecular distributions, sources and transformation, Atmospheric Research, 170, 140–160, https://doi.org/10.1016/j.atmosres.2015.11.018, 2016.

Kawamura, K. and Gagosian, R. B.: Implications of ω-oxocarboxylic acids in the remote marine atmosphere for photo-oxidation of unsaturated fatty acids, Nature, 325, 330–332, https://doi.org/10.1038/325330a0, 1987.

Kawamura, K. and Ikushima, K.: Seasonal changes in the distribution of dicarboxylic acids in the urban atmosphere, Environ. Sci. Technol., 27, 2227–2235, https://doi.org/10.1021/es00047a033, 1993.

Kawamura, K. and Sakaguchi, F.: Molecular distributions of water soluble dicarboxylic acids in marine aerosols over the Pacific Ocean including tropics, Journal of Geophysical Research: Atmospheres, 104, 3501–3509, https://doi.org/10.1029/1998JD100041, 1999.

Kawana, K., Miyazaki, Y., Omori, Y., Tanimoto, H., Kagami, S., Suzuki, K., Yamashita, Y., Nishioka, J., Deng, Y., Yai, H., and Mochida, M.: Number-Size Distribution and CCN Activity of Atmospheric Aerosols in the Western North Pacific During Spring Pre-Bloom Period: Influences of Terrestrial and Marine Sources, Journal of Geophysical Research: Atmospheres, 127, e2022JD036690, https://doi.org/10.1029/2022JD036690, 2022.

Kleindienst, T. E., Jaoui, M., Lewandowski, M., Offenberg, J. H., Lewis, C. W., Bhave, P. V., and Edney, E. O.: Estimates of the contributions of biogenic and anthropogenic hydrocarbons to secondary organic aerosol at a southeastern US location, Atmospheric Environment, 41, 8288–8300, https://doi.org/10.1016/j.atmosenv.2007.06.045, 2007.

Kleindienst, T. E., Jaoui, M., Lewandowski, M., Offenberg, J. H., and Docherty, K. S.: The formation of SOA and chemical tracer compounds from the photooxidation of naphthalene and its methyl analogs in the presence and absence of nitrogen oxides, Atmospheric Chemistry and Physics, 12, 8711–8726, https://doi.org/10.5194/acp-12-8711-2012, 2012.

Le, T., Wang, Y., Liu, L., Yang, J., Yung, Y. L., Li, G., and Seinfeld, J. H.: Unexpected air pollution with marked emission reductions during the COVID-19 outbreak in China, Science, 369, 702–706, https://doi.org/10.1126/science.abb7431, 2020.

Li, B., Zhang, J., Zhao, Y., Yuan, S., Zhao, Q., Shen, G., and Wu, H.: Seasonal variation of urban carbonaceous aerosols in a typical city Nanjing in Yangtze River Delta, China, Atmospheric Environment, 106, 223–231, https://doi.org/10.1016/j.atmosenv.2015.01.064, 2015.

Li, C., Bosch, C., Kang, S., Andersson, A., Chen, P., Zhang, Q., Cong, Z., Chen, B., Qin, D., and Gustafsson, Ö.: Sources of black carbon to the Himalayan–Tibetan Plateau glaciers, Nature Communications, 7, 12574, https://doi.org/10.1038/ncomms12574, 2016a.

Li, F., Tsona, N. T., Li, J., and Du, L.: Aqueous-phase oxidation of syringic acid emitted from biomass burning: Formation of light-absorbing compounds, Science of The Total Environment, 765, 144239, https://doi.org/10.1016/j.scitotenv.2020.144239, 2021a.

Li, H., Wang, Q., Yang, M., Li, F., Wang, J., Sun, Y., Wang, C., Wu, H., and Qian, X.: Chemical characterization and source apportionment of PM2.5 aerosols in a megacity of Southeast China, Atmospheric Research, 181, 288–299, https://doi.org/10.1016/j.atmosres.2016.07.005, 2016b.

Li, J. J., Wang, G. H., Cao, J. J., Wang, X. M., and Zhang, R. J.: Observation of biogenic secondary organic aerosols in the atmosphere of a mountain site in central China: temperature and relative humidity effects, Atmospheric Chemistry and Physics, 13, 11535–11549, https://doi.org/10.5194/acp-13-11535-2013, 2013.

Li, K., Zhang, J., Bell, D. M., Wang, T., Lamkaddam, H., Cui, T., Qi, L., Surdu, M., Wang, D., Du, L., El Haddad, I., Slowik, J. G., and Prevot, A. S. H.: Uncovering the dominant contribution of intermediate volatility compounds in secondary organic aerosol formation from biomass-burning emissions, National Science Review, 11, nwae014, https://doi.org/10.1093/nsr/nwae014, 2024.

Li, L., Ren, L., Ren, H., Yue, S., Xie, Q., Zhao, W., Kang, M., Li, J., Wang, Z., Sun, Y., and Fu, P.: Molecular Characterization and Seasonal Variation in Primary and Secondary Organic Aerosols in Beijing, China, Journal of Geophysical Research: Atmospheres, 123, 12,394-12,412, https://doi.org/10.1029/2018JD028527, 2018.

Li, X.-B., Yuan, B., Wang, S., Wang, C., Lan, J., Liu, Z., Song, Y., He, X., Huangfu, Y., Pei, C., Cheng, P., Yang, S., Qi, J., Wu, C., Huang, S., You, Y., Chang, M., Zheng, H., Yang, W., Wang, X., and Shao, M.: Variations and sources of volatile organic compounds (VOCs) in urban region: insights from measurements on a tall tower, Atmospheric Chemistry and Physics, 22, 10567–10587, https://doi.org/10.5194/acp-22-10567-2022, 2022.

Li, Y., Fu, T.-M., Yu, J. Z., Feng, X., Zhang, L., Chen, J., Boreddy, S. K. R., Kawamura, K., Fu, P., Yang, X., Zhu, L., and Zeng, Z.: Impacts of Chemical Degradation on the Global Budget of Atmospheric Levoglucosan and Its Use As a Biomass Burning Tracer, Environ. Sci. Technol., 55, 5525–5536, https://doi.org/10.1021/acs.est.0c07313, 2021b.

Li, Y. J., Huang, D. D., Cheung, H. Y., Lee, A. K. Y., and Chan, C. K.: Aqueous-phase photochemical oxidation and direct photolysis of vanillin – a model compound of methoxy phenols from biomass burning, Atmospheric Chemistry and Physics, 14, 2871–2885, https://doi.org/10.5194/acp-14-2871-2014, 2014.

Lim, C. Y., Hagan, D. H., Coggon, M. M., Koss, A. R., Sekimoto, K., de Gouw, J., Warneke, C., Cappa, C. D., and Kroll, J. H.: Secondary organic aerosol formation from the laboratory oxidation of biomass burning emissions, Atmospheric Chemistry and Physics, 19, 12797–12809, https://doi.org/10.5194/acp-19-12797-2019, 2019.

Limbeck, A., Puxbaum, H., Otter, L., and Scholes, M. C.: Semivolatile behavior of dicarboxylic acids and other polar organic species at a rural background site (Nylsvley, RSA), Atmospheric Environment, 35, 1853–1862, https://doi.org/10.1016/S1352-2310(00)00497-0, 2001.

Lin, Y.-C., Zhang, Y.-L., Fan, M.-Y., and Bao, M.: Heterogeneous formation of particulate nitrate under ammonium-rich regimes during the high-$PM_{2.5}$ events in Nanjing, China,

Atmospheric Chemistry and Physics, 20, 3999–4011, https://doi.org/10.5194/acp-20-3999-2020, 2020.

Lin, Y.-C., Fan, M.-Y., Hong, Y., Yu, M., Cao, F., and Zhang, Y.-L.: Important contributions of natural gas combustion to atmospheric nitrate aerosols in China: Insights from stable nitrogen isotopes, Science Bulletin, https://doi.org/10.1016/j.scib.2024.06.038, 2024.

Lin, Y.-H., Zhang, H., Pye, H. O. T., Zhang, Z., Marth, W. J., Park, S., Arashiro, M., Cui, T., Budisulistiorini, S. H., Sexton, K. G., Vizuete, W., Xie, Y., Luecken, D. J., Piletic, I. R., Edney, E. O., Bartolotti, L. J., Gold, A., and Surratt, J. D.: Epoxide as a precursor to secondary organic aerosol formation from isoprene photooxidation in the presence of nitrogen oxides, Proceedings of the National Academy of Sciences, 110, 6718–6723, https://doi.org/10.1073/pnas.1221150110, 2013a.

Lin, Y.-H., Knipping, E. M., Edgerton, E. S., Shaw, S. L., and Surratt, J. D.: Investigating the influences of SO_2 and NH_3 levels on isoprene-derived secondary organic aerosol formation using conditional sampling approaches, Atmospheric Chemistry and Physics, 13, 8457–8470, https://doi.org/10.5194/acp-13-8457-2013, 2013b.

Liu, D., Li, J., Zhang, Y., Xu, Y., Liu, X., Ding, P., Shen, C., Chen, Y., Tian, C., and Zhang, G.: The Use of Levoglucosan and Radiocarbon for Source Apportionment of PM2.5 Carbonaceous Aerosols at a Background Site in East China, Environ. Sci. Technol., 47, 10454–10461, https://doi.org/10.1021/es401250k, 2013.

Liu, J., Li, J., Zhang, Y., Liu, D., Ding, P., Shen, C., Shen, K., He, Q., Ding, X., Wang, X., Chen, D., Szidat, S., and Zhang, G.: Source Apportionment Using Radiocarbon and Organic Tracers for PM2.5 Carbonaceous Aerosols in Guangzhou, South China: Contrasting Local- and Regional-Scale Haze Events, Environ. Sci. Technol., 48, 12002–12011, https://doi.org/10.1021/es503102w, 2014.

Liu, J., Li, J., Liu, D., Ding, P., Shen, C., Mo, Y., Wang, X., Luo, C., Cheng, Z., Szidat, S., Zhang, Y., Chen, Y., and Zhang, G.: Source apportionment and dynamic changes of carbonaceous aerosols during the haze bloom-decay process in China based on radiocarbon and organic molecular tracers, Atmospheric Chemistry and Physics, 16, 2985–2996, https://doi.org/10.5194/acp-16-2985-2016, 2016.

Liu, J., Zhou, S., Zhang, Z., Kawamura, K., Zhao, W., Wang, X., Shao, M., Jiang, F., Liu, J., Sun, X., Hang, J., Zhao, J., Pei, C., Zhang, J., and Fu, P.: Characterization of dicarboxylic acids, oxoacids, and α-dicarbonyls in PM2.5 within the urban boundary layer in southern China: Sources and formation pathways, Environmental Pollution, 285, 117185, https://doi.org/10.1016/j.envpol.2021.117185, 2021.

Lu, K., Guo, S., Tan, Z., Wang, H., Shang, D., Liu, Y., Li, X., Wu, Z., Hu, M., and Zhang, Y.: Exploring atmospheric free-radical chemistry in China: the self-cleansing capacity and the formation of secondary air pollution, National Science Review, 6, 579–594, https://doi.org/10.1093/nsr/nwy073, 2019.

Medeiros, P. M., Conte, M. H., Weber, J. C., and Simoneit, B. R. T.: Sugars as source indicators of biogenic organic carbon in aerosols collected above the Howland Experimental Forest, Maine, Atmospheric Environment, 40, 1694–1705, https://doi.org/10.1016/j.atmosenv.2005.11.001, 2006.

Mochida, M., Kawabata, A., Kawamura, K., Hatsushika, H., and Yamazaki, K.: Seasonal variation and origins of dicarboxylic acids in the marine atmosphere over the western

North Pacific, Journal of Geophysical Research: Atmospheres, 108, https://doi.org/10.1029/2002JD002355, 2003.
Mochida, M., Kawamura, K., Fu, P., and Takemura, T.: Seasonal variation of levoglucosan in aerosols over the western North Pacific and its assessment as a biomass-burning tracer, Atmospheric Environment, 44, 3511–3518, https://doi.org/10.1016/j.atmosenv.2010.06.017, 2010.
Morris, C. E., Sands, D. C., Bardin, M., Jaenicke, R., Vogel, B., Leyronas, C., Ariya, P. A., and Psenner, R.: Microbiology and atmospheric processes: research challenges concerning the impact of airborne micro-organisms on the atmosphere and climate, Biogeosciences, 8, 17–25, https://doi.org/10.5194/bg-8-17-2011, 2011.
Mozaffar, A., Zhang, Y.-L., Fan, M., Cao, F., and Lin, Y.-C.: Characteristics of summertime ambient VOCs and their contributions to O3 and SOA formation in a suburban area of Nanjing, China, Atmospheric Research, 240, 104923, https://doi.org/10.1016/j.atmosres.2020.104923, 2020.
Pope, C. A., Burnett, R. T., Thurston, G. D., Thun, M. J., Calle, E. E., Krewski, D., and Godleski, J. J.: Cardiovascular Mortality and Long-Term Exposure to Particulate Air Pollution, Circulation, 109, 71–77, https://doi.org/10.1161/01.CIR.0000108927.80044.7F, 2004.
Pöschl, U., Martin, S. T., Sinha, B., Chen, Q., Gunthe, S. S., Huffman, J. A., Borrmann, S., Farmer, D. K., Garland, R. M., Helas, G., Jimenez, J. L., King, S. M., Manzi, A., Mikhailov, E., Pauliquevis, T., Petters, M. D., Prenni, A. J., Roldin, P., Rose, D., Schneider, J., Su, H., Zorn, S. R., Artaxo, P., and Andreae, M. O.: Rainforest Aerosols as Biogenic Nuclei of Clouds and Precipitation in the Amazon, Science, 329, 1513–1516, https://doi.org/10.1126/science.1191056, 2010.
Puxbaum, H. and Tenze-Kunit, M.: Size distribution and seasonal variation of atmospheric cellulose, Atmospheric Environment, 37, 3693–3699, https://doi.org/10.1016/S1352-2310(03)00451-5, 2003.
Ram, K., Sarin, M. M., and Hegde, P.: Long-term record of aerosol optical properties and chemical composition from a high-altitude site (Manora Peak) in Central Himalaya, Atmospheric Chemistry and Physics, 10, 11791–11803, https://doi.org/10.5194/acp-10-11791-2010, 2010.
Ren, G., Yan, X., Ma, Y., Qiao, L., Chen, Z., Xin, Y., Zhou, M., Shi, Y., Zheng, K., Zhu, S., Huang, C., and Li, L.: Characteristics and source apportionment of PM2.5-bound saccharides and carboxylic acids in Central Shanghai, China, Atmospheric Research, 237, 104817, https://doi.org/10.1016/j.atmosres.2019.104817, 2020.
Rivellini, L.-H., Jorga, S., Wang, Y., Lee, A. K. Y., Murphy, J. G., Chan, A. W., and Abbatt, J. P. D.: Sources of Wintertime Atmospheric Organic Pollutants in a Large Canadian City: Insights from Particle and Gas Phase Measurements, ACS EST Air, https://doi.org/10.1021/acsestair.4c00039, 2024.
Rogge, W. F., Hildemann, L. M., Mazurek, M. A., Cass, G. R., and Simoneit, B. R. T.: Sources of fine organic aerosol. 2. Noncatalyst and catalyst-equipped automobiles and heavy-duty diesel trucks, Environ. Sci. Technol., 27, 636–651, https://doi.org/10.1021/es00041a007, 1993.
Rogge, W. F., Medeiros, P. M., and Simoneit, B. R. T.: Organic marker compounds in surface soils of crop fields from the San Joaquin Valley fugitive dust characterization study,

Atmospheric Environment, 41, 8183–8204, https://doi.org/10.1016/j.atmosenv.2007.06.030, 2007.

Saxena, P. and Hildemann, L. M.: Water-soluble organics in atmospheric particles: A critical review of the literature and application of thermodynamics to identify candidate compounds, J Atmos Chem, 24, 57–109, https://doi.org/10.1007/BF00053823, 1996.

Shah, V., Keller, C. A., Knowland, K. E., Christiansen, A., Hu, L., Wang, H., Lu, X., Alexander, B., and Jacob, D. J.: Particulate Nitrate Photolysis as a Possible Driver of Rising Tropospheric Ozone, Geophysical Research Letters, 51, e2023GL107980, https://doi.org/10.1029/2023GL107980, 2024.

Sharkey, T. D., Wiberley, A. E., and Donohue, A. R.: Isoprene Emission from Plants: Why and How, Ann Bot, 101, 5–18, https://doi.org/10.1093/aob/mcm240, 2008.

Simoneit, B. R. T.: Biomass burning — a review of organic tracers for smoke from incomplete combustion, Applied Geochemistry, 17, 129–162, https://doi.org/10.1016/S0883-2927(01)00061-0, 2002.

Simoneit, B. R. T., Kobayashi, M., Mochida, M., Kawamura, K., and Huebert, B. J.: Aerosol particles collected on aircraft flights over the northwestern Pacific region during the ACE-Asia campaign: Composition and major sources of the organic compounds, Journal of Geophysical Research: Atmospheres, 109, https://doi.org/10.1029/2004JD004565, 2004a.

Simoneit, B. R. T., Elias, V. O., Kobayashi, M., Kawamura, K., Rushdi, A. I., Medeiros, P. M., Rogge, W. F., and Didyk, B. M.: SugarsDominant Water-Soluble Organic Compounds in Soils and Characterization as Tracers in Atmospheric Particulate Matter, Environ. Sci. Technol., 38, 5939–5949, https://doi.org/10.1021/es0403099, 2004b.

Sindelarova, K., Granier, C., Bouarar, I., Guenther, A., Tilmes, S., Stavrakou, T., Müller, J.-F., Kuhn, U., Stefani, P., and Knorr, W.: Global data set of biogenic VOC emissions calculated by the MEGAN model over the last 30 years, Atmospheric Chemistry and Physics, 14, 9317–9341, https://doi.org/10.5194/acp-14-9317-2014, 2014.

Song, W., Zhang, Y.-L., Zhang, Y., Cao, F., Rauber, M., Salazar, G., Kawichai, S., Prapamontol, T., and Szidat, S.: Is biomass burning always a dominant contributor of fine aerosols in upper northern Thailand?, Environment International, 168, 107466, https://doi.org/10.1016/j.envint.2022.107466, 2022.

Srivastava, D., Vu, T. V., Tong, S., Shi, Z., and Harrison, R. M.: Formation of secondary organic aerosols from anthropogenic precursors in laboratory studies, npj Clim Atmos Sci, 5, 1–30, https://doi.org/10.1038/s41612-022-00238-6, 2022.

Suh, I., Zhang, R., Molina, L. T., and Molina, M. J.: Oxidation Mechanism of Aromatic Peroxy and Bicyclic Radicals from OH−Toluene Reactions, J. Am. Chem. Soc., 125, 12655–12665, https://doi.org/10.1021/ja0350280, 2003.

Sullivan, A. P., Holden, A. S., Patterson, L. A., McMeeking, G. R., Kreidenweis, S. M., Malm, W. C., Hao, W. M., Wold, C. E., and Collett Jr., J. L.: A method for smoke marker measurements and its potential application for determining the contribution of biomass burning from wildfires and prescribed fires to ambient PM2.5 organic carbon, Journal of Geophysical Research: Atmospheres, 113, https://doi.org/10.1029/2008JD010216, 2008.

Sun, Y., Jiang, Q., Wang, Z., Fu, P., Li, J., Yang, T., and Yin, Y.: Investigation of the sources and evolution processes of severe haze pollution in Beijing in January 2013, Journal of

Geophysical Research: Atmospheres, 119, 4380–4398, https://doi.org/10.1002/2014JD021641, 2014.

Surratt, J. D., Murphy, S. M., Kroll, J. H., Ng, N. L., Hildebrandt, L., Sorooshian, A., Szmigielski, R., Vermeylen, R., Maenhaut, W., Claeys, M., Flagan, R. C., and Seinfeld, J. H.: Chemical Composition of Secondary Organic Aerosol Formed from the Photooxidation of Isoprene, J. Phys. Chem. A, 110, 9665–9690, https://doi.org/10.1021/jp061734m, 2006.

Surratt, J. D., Chan, A. W. H., Eddingsaas, N. C., Chan, M., Loza, C. L., Kwan, A. J., Hersey, S. P., Flagan, R. C., Wennberg, P. O., and Seinfeld, J. H.: Reactive intermediates revealed in secondary organic aerosol formation from isoprene, Proceedings of the National Academy of Sciences, 107, 6640–6645, https://doi.org/10.1073/pnas.0911114107, 2010.

Urban, R. C., Lima-Souza, M., Caetano-Silva, L., Queiroz, M. E. C., Nogueira, R. F. P., Allen, A. G., Cardoso, A. A., Held, G., and Campos, M. L. A. M.: Use of levoglucosan, potassium, and water-soluble organic carbon to characterize the origins of biomass-burning aerosols, Atmospheric Environment, 61, 562–569, https://doi.org/10.1016/j.atmosenv.2012.07.082, 2012.

Virkkula, A., Teinilä, K., Hillamo, R., Kerminen, V.-M., Saarikoski, S., Aurela, M., Viidanoja, J., Paatero, J., Koponen, I. K., and Kulmala, M.: Chemical composition of boundary layer aerosol over the Atlantic Ocean and at an Antarctic site, Atmospheric Chemistry and Physics, 6, 3407–3421, https://doi.org/10.5194/acp-6-3407-2006, 2006.

Wang, G., Kawamura, K., Lee, S., Ho, K., and Cao, J.: Molecular, Seasonal, and Spatial Distributions of Organic Aerosols from Fourteen Chinese Cities, Environ. Sci. Technol., 40, 4619–4625, https://doi.org/10.1021/es060291x, 2006.

Wang, L., Li, Q., Qiu, Q., Hou, L., Ouyang, J., Zeng, R., Huang, S., Li, J., Tang, L., and Liu, Y.: Assessing the ecological risk induced by PM2.5 pollution in a fast developing urban agglomeration of southeastern China, Journal of Environmental Management, 324, 116284, https://doi.org/10.1016/j.jenvman.2022.116284, 2022.

Wang, P., Chen, K., Zhu, S., Wang, P., and Zhang, H.: Severe air pollution events not avoided by reduced anthropogenic activities during COVID-19 outbreak, Resources, Conservation and Recycling, 158, 104814, https://doi.org/10.1016/j.resconrec.2020.104814, 2020.

Wu, X., Cao, F., Haque, M., Fan, M.-Y., Zhang, S.-C., and Zhang, Y.-L.: Molecular composition and source apportionment of fine organic aerosols in Northeast China, Atmospheric Environment, 239, 117722, https://doi.org/10.1016/j.atmosenv.2020.117722, 2020.

Xiao, Y., Hu, M., Li, X., Zong, T., Xu, N., Hu, S., Zeng, L., Chen, S., Song, Y., Guo, S., and Wu, Z.: Aqueous secondary organic aerosol formation attributed to phenols from biomass burning, Science of The Total Environment, 847, 157582, https://doi.org/10.1016/j.scitotenv.2022.157582, 2022.

Yan, C., Tham, Y. J., Nie, W., Xia, M., Wang, H., Guo, Y., Ma, W., Zhan, J., Hua, C., Li, Y., Deng, C., Li, Y., Zheng, F., Chen, X., Li, Q., Zhang, G., Mahajan, A. S., Cuevas, C. A., Huang, D. D., Wang, Z., Sun, Y., Saiz-Lopez, A., Bianchi, F., Kerminen, V.-M., Worsnop, D. R., Donahue, N. M., Jiang, J., Liu, Y., Ding, A., and Kulmala, M.: Increasing contribution of nighttime nitrogen chemistry to wintertime haze formation in Beijing observed during COVID-19 lockdowns, Nat. Geosci., 1–7, https://doi.org/10.1038/s41561-023-01285-1, 2023.

Yang, G.-P., Zhang, S.-H., Zhang, H.-H., Yang, J., and Liu, C.-Y.: Distribution of biogenic sulfur in the Bohai Sea and northern Yellow Sea and its contribution to atmospheric sulfate aerosol in the late fall, Marine Chemistry, 169, 23–32, https://doi.org/10.1016/j.marchem.2014.12.008, 2015.

Yang, T., Li, H., Xu, W., Song, Y., Xu, L., Wang, H., Wang, F., Sun, Y., Wang, Z., and Fu, P.: Strong Impacts of Regional Atmospheric Transport on the Vertical Distribution of Aerosol Ammonium over Beijing, Environ. Sci. Technol. Lett., 11, 29–34, https://doi.org/10.1021/acs.estlett.3c00791, 2024.

Yang, Y., Chan, C., Tao, J., Lin, M., Engling, G., Zhang, Z., Zhang, T., and Su, L.: Observation of elevated fungal tracers due to biomass burning in the Sichuan Basin at Chengdu City, China, Science of The Total Environment, 431, 68–77, https://doi.org/10.1016/j.scitotenv.2012.05.033, 2012.

Yee, L. D., Kautzman, K. E., Loza, C. L., Schilling, K. A., Coggon, M. M., Chhabra, P. S., Chan, M. N., Chan, A. W. H., Hersey, S. P., Crounse, J. D., Wennberg, P. O., Flagan, R. C., and Seinfeld, J. H.: Secondary organic aerosol formation from biomass burning intermediates: phenol and methoxyphenols, Atmospheric Chemistry and Physics, 13, 8019–8043, https://doi.org/10.5194/acp-13-8019-2013, 2013.

Youn, J.-S., Wang, Z., Wonaschütz, A., Arellano, A., Betterton, E. A., and Sorooshian, A.: Evidence of aqueous secondary organic aerosol formation from biogenic emissions in the North American Sonoran Desert, Geophysical Research Letters, 40, 3468–3472, https://doi.org/10.1002/grl.50644, 2013.

Zhang, H., Li, J., Ying, Q., Yu, J. Z., Wu, D., Cheng, Y., He, K., and Jiang, J.: Source apportionment of PM2.5 nitrate and sulfate in China using a source-oriented chemical transport model, Atmospheric Environment, 62, 228–242, https://doi.org/10.1016/j.atmosenv.2012.08.014, 2012.

Zhang, H., Hu, J., Kleeman, M., and Ying, Q.: Source apportionment of sulfate and nitrate particulate matter in the Eastern United States and effectiveness of emission control programs, Science of The Total Environment, 490, 171–181, https://doi.org/10.1016/j.scitotenv.2014.04.064, 2014a.

Zhang, J., He, X., Ding, X., Yu, J. Z., and Ying, Q.: Modeling Secondary Organic Aerosol Tracers and Tracer-to-SOA Ratios for Monoterpenes and Sesquiterpenes Using a Chemical Transport Model, Environ. Sci. Technol., 56, 804–813, https://doi.org/10.1021/acs.est.1c06373, 2022.

Zhang, J., Liu, J., Ding, X., He, X., Zhang, T., Zheng, M., Choi, M., Isaacman-VanWertz, G., Yee, L., Zhang, H., Misztal, P., Goldstein, A. H., Guenther, A. B., Budisulistiorini, S. H., Surratt, J. D., Stone, E. A., Shrivastava, M., Wu, D., Yu, J. Z., and Ying, Q.: New formation and fate of Isoprene SOA markers revealed by field data-constrained modeling, npj Clim Atmos Sci, 6, 1–8, https://doi.org/10.1038/s41612-023-00394-3, 2023.

Zhang, J., Shrivastava, M., Ma, L., Jiang, W., Anastasio, C., Zhang, Q., and Zelenyuk, A.: Modeling Novel Aqueous Particle and Cloud Chemistry Processes of Biomass Burning Phenols and Their Potential to Form Secondary Organic Aerosols, Environ. Sci. Technol., 58, 3776–3786, https://doi.org/10.1021/acs.est.3c07762, 2024.

Zhang, T., Claeys, M., Cachier, H., Dong, S., Wang, W., Maenhaut, W., and Liu, X.: Identification and estimation of the biomass burning contribution to Beijing aerosol using

levoglucosan as a molecular marker, Atmospheric Environment, 42, 7013–7021, https://doi.org/10.1016/j.atmosenv.2008.04.050, 2008.

Zhang, Y., Huang, J.-P., Henze, D. K., and Seinfeld, J. H.: Role of isoprene in secondary organic aerosol formation on a regional scale, Journal of Geophysical Research: Atmospheres, 112, https://doi.org/10.1029/2007JD008675, 2007.

Zhang, Y., Ren, H., Sun, Y., Cao, F., Chang, Y., Liu, S., Lee, X., Agrios, K., Kawamura, K., Liu, D., Ren, L., Du, W., Wang, Z., Prévôt, A. S. H., Szidat, S., and Fu, P.: High Contribution of Nonfossil Sources to Submicrometer Organic Aerosols in Beijing, China, Environ. Sci. Technol., 51, 7842–7852, https://doi.org/10.1021/acs.est.7b01517, 2017.

Zhang, Y.-L., Li, J., Zhang, G., Zotter, P., Huang, R.-J., Tang, J.-H., Wacker, L., Prévôt, A. S. H., and Szidat, S.: Radiocarbon-Based Source Apportionment of Carbonaceous Aerosols at a Regional Background Site on Hainan Island, South China, Environ. Sci. Technol., 48, 2651–2659, https://doi.org/10.1021/es4050852, 2014b.

Zhang, Y.-L., Huang, R.-J., El Haddad, I., Ho, K.-F., Cao, J.-J., Han, Y., Zotter, P., Bozzetti, C., Daellenbach, K. R., Canonaco, F., Slowik, J. G., Salazar, G., Schwikowski, M., Schnelle-Kreis, J., Abbaszade, G., Zimmermann, R., Baltensperger, U., Prévôt, A. S. H., and Szidat, S.: Fossil vs. non-fossil sources of fine carbonaceous aerosols in four Chinese cities during the extreme winter haze episode of 2013, Atmospheric Chemistry and Physics, 15, 1299–1312, https://doi.org/10.5194/acp-15-1299-2015, 2015.

Zhang, Y.-L., Kawamura, K., Agrios, K., Lee, M., Salazar, G., and Szidat, S.: Fossil and Nonfossil Sources of Organic and Elemental Carbon Aerosols in the Outflow from Northeast China, Environ. Sci. Technol., 50, 6284–6292, https://doi.org/10.1021/acs.est.6b00351, 2016.

Zhang, Y.-L., El-Haddad, I., Huang, R.-J., Ho, K.-F., Cao, J.-J., Han, Y., Zotter, P., Bozzetti, C., Daellenbach, K. R., Slowik, J. G., Salazar, G., Prévôt, A. S. H., and Szidat, S.: Large contribution of fossil fuel derived secondary organic carbon to water soluble organic aerosols in winter haze in China, Atmospheric Chemistry and Physics, 18, 4005–4017, https://doi.org/10.5194/acp-18-4005-2018, 2018.

Zhu, C., Kawamura, K., and Kunwar, B.: Effect of biomass burning over the western North Pacific Rim: wintertime maxima of anhydrosugars in ambient aerosols from Okinawa, Atmospheric Chemistry and Physics, 15, 1959–1973, https://doi.org/10.5194/acp-15-1959-2015, 2015a.

Zhu, C., Kawamura, K., and Kunwar, B.: Organic tracers of primary biological aerosol particles at subtropical Okinawa Island in the western North Pacific Rim, Journal of Geophysical Research: Atmospheres, 120, 5504–5523, https://doi.org/10.1002/2015JD023611, 2015b.

Table 1. Concentrations of $PM_{2.5}$ components in aerosol samples collected in urban Nanjing during polluted episodes.

$PM_{2.5}$ ($\mu g\ m^{-3}$)	>200				100-200				<100			
Species	mean	std	min	max	mean	std	min	max	mean	std	min	max
EC ($\mu g\ m^{-3}$)	2.67	0.26	2.27	3.08	2.00	0.08	1.93	2.14	1.73	0.31	1.26	2.24
OC ($\mu g\ m^{-3}$)	35.4	4.78	23.8	41.1	23.7	3.86	18.5	28.7	15.3	6.19	8.74	26.7
TC ($\mu g\ m^{-3}$)	38.1	4.85	26.0	43.4	25.7	3.91	20.5	30.7	17.0	6.39	10.2	28.8
WSOC ($\mu g\ m^{-3}$)	14.3	2.62	8.97	18.1	10.2	1.30	8.11	11.4	6.21	1.90	3.84	8.26
WISOC ($\mu g\ m^{-3}$)	21.1	3.68	14.8	25.8	13.5	2.78	10.4	17.5	9.87	4.64	4.55	19.4
OC/EC	13.3	2.08	10.5	17.4	11.8	1.74	9.57	14.4	8.70	2.72	6.00	13.2
WSOC/OC	0.40	0.06	0.31	0.49	0.43	0.03	0.39	0.47	0.35	0.17	nd	0.51
WISOC/OC	0.60	0.06	0.51	0.69	0.57	0.03	0.53	0.61	0.65	0.17	0.49	1.00
14C-WSOC	0.31	0.06	0.25	0.39	0.25	0.02	0.23	0.28	0.24	0.04	0.18	0.29
Inorganic icons ($\mu g\ m^{-3}$)												
F^-	0.08	0.03	0.05	0.12	0.16	0.20	0.06	0.52	0.05	0.02	0.02	0.08
Cl^-	7.00	1.66	3.86	10.2	6.51	1.50	4.26	7.86	5.51	2.62	1.88	10.2
NO_3^-	56.0	4.39	48.7	62.4	33.9	6.50	24.0	40.1	12.7	4.37	5.75	17.7

SO_4^{2-}	30.9	4.42	26.4	38.8	19.1	3.78	13.2	23.8	10.4	3.95	6.59	19.4
NH_4^+	28.0	3.20	20.3	30.9	17.1	3.60	10.8	19.7	8.52	2.35	4.97	11.4
PO_4^{3-}	0.14	0.02	0.11	0.17	0.07	0.03	0.03	0.12	0.02	0.01	0.01	0.03
Na^+	0.73	0.15	0.47	0.98	0.83	0.18	0.59	1.08	0.47	0.16	0.29	0.76
Ca^{2+}	0.73	0.41	0.35	1.58	1.23	0.55	0.76	1.99	0.40	0.16	0.19	0.62
nss-Ca^{2+}	0.70	0.41	0.32	1.55	1.20	0.55	0.73	1.96	0.38	0.16	0.17	0.61
K^+	0.98	0.24	0.72	1.52	1.01	0.34	0.62	1.40	0.65	0.48	0.22	1.69
nss-K^+	0.95	0.24	0.69	1.49	0.98	0.34	0.60	1.36	0.64	0.48	0.21	1.67
Mg^{2+}	0.69	0.37	0.25	1.18	0.24	0.14	0.10	0.42	0.10	0.07	0.03	0.22
Anhydrosugars (ng m^{-3})												
Levoglucosan (L)	471	122	284	721	185	28.1	142	219	201	121	59.0	395
Galactosan (G)	39.6	19.1	4.84	63.6	73.2	14.8	55.1	94.1	51.0	44.6	6.70	115
Mannosan (M)	45.4	21.2	20.8	81.9	14.8	9.73	4.79	30.3	14.0	8.11	6.63	25.4
L/M	11.5	3.21	5.86	16.5	18.3	12.4	4.67	38.0	22.4	12.7	8.88	38.2
M/G	2.86	4.83	0.41	15.6	0.20	0.13	0.07	0.41	0.66	1.20	nd	3.09
L/K^+	0.51	0.19	0.21	0.76	0.20	0.07	0.14	0.29	0.44	0.33	0.06	1.04
Sugar alcohol (ng m^{-3})												

arabitol	30.5	10.3	12.0	44.1	28.8	10.4	16.6	42.1	17.8	13.4	4.59	48.2
mannitol	14.4	6.24	0.47	24.4	14.2	4.12	7.92	18.4	12.9	7.20	2.43	22.0
glycerol	295	151	119	561	1822	1916	376	4062	2348	1334	652	4749
Sugars (ng m^{-3})												
trehalose	851	874	86.5	2970	1057	1112	302	3023	672	521	257	1378
glucose	203	85.1	49.3	377	312	148	193	551	158	56.0	69.8	240
total measured saccharides	1951	896	633	3841	3507	1632	1738	4976	3474	1238	1478	5436
Isoprene SOA tracers (ng m^{-3})												
cis-2-methyl-1,3,4-trihydroxy-1-butene	0.38	0.42	0.02	1.26	0.62	0.17	0.38	0.85	0.36	0.17	0.11	0.68
3-methyl-2,3,4-trihydroxy-1-butene	0.45	0.67	0.03	2.17	0.59	0.24	0.26	0.93	0.64	0.37	0.01	1.07
trans-2-methyl-1,3,4-trihydroxy-1-butene	0.76	0.83	0.03	2.87	0.99	0.53	0.41	1.81	0.74	0.52	0.06	1.55
sum of C5-Alkene triols	1.59	1.83	0.07	6.30	2.20	0.56	1.66	2.91	1.74	0.99	0.18	3.19
2-methylthreitol	0.69	1.16	0.07	3.78	1.52	0.60	0.65	2.26	1.16	0.92	0.03	3.11
2-methylerythitol	1.17	1.55	0.10	4.93	2.30	0.69	1.29	2.97	2.10	1.19	0.41	4.30

sum of 2-methyltetrols	1.86	2.68	0.20	8.71	3.81	1.20	1.94	4.67	3.26	2.09	0.45	7.41
2-methylglyceric acid	2.05	1.86	0.21	5.93	2.56	0.96	1.13	3.52	1.58	1.09	0.35	3.80
sum of isoprene SOA	5.51	6.23	0.56	20.9	8.58	2.52	4.80	11.1	6.58	4.10	0.97	14.4
Monoterpene SOA tracers (ng m^{-3})												
3HGA	2.45	1.64	0.94	5.52	2.75	2.30	1.02	6.60	0.95	0.39	0.42	1.53
pinonic	1.61	2.15	0.05	6.91	3.41	1.67	1.65	5.64	1.04	0.57	0.38	1.81
pinic	0.32	0.31	0.05	1.06	0.87	0.62	0.24	1.81	0.84	0.69	0.04	1.69
sum of monoterpene SOA	4.38	4.00	1.17	13.5	7.03	3.79	3.22	12.7	2.82	0.90	1.36	4.09
Sesquiterpene SOA tracers (ng m^{-3})												
β-caryophylinic acid	0.26	0.38	nd	1.03	0.22	0.42	nd	0.97	0.29	0.45	nd	1.33
total measured biogenic SOA tracers	10.2	10.2	1.80	34.7	15.8	5.75	8.14	24.3	9.69	4.92	2.36	18.6
Saturated dicarboxylic acids (µg m^{-3})												
oxalic acid, C2	0.46	0.16	0.23	0.74	0.34	0.11	0.23	0.51	0.18	0.06	0.09	0.30
malonic acid, C3	6.43	2.10	1.51	8.71	10.0	2.41	8.50	14.3	5.96	2.41	1.48	8.14
succinic Acid, C4	0.04	0.02	0.01	0.07	0.03	0.02	0.01	0.06	0.01	0.01	nd	0.02
glutaric acid, C5	0.06	0.02	0.03	0.08	0.04	0.02	0.02	0.06	0.02	0.01	0.01	0.03

sum of saturated diacids	6.99	2.10	1.96	9.19	10.4	2.34	9.12	14.6	6.16	2.41	1.66	8.32
Unsaturated aliphatic diacids (ng m^{-3})												
maleic acid	8.32	5.35	0.86	20.2	21.3	9.11	11.5	33.1	10.79	13.1	1.00	41.9
fumaric acid	11.7	6.84	1.61	27.6	15.5	5.34	8.32	23.2	11.51	8.01	1.70	27.6
M/F	0.71	0.28	0.27	1.26	1.38	0.35	0.80	1.72	0.85	0.44	0.32	1.52
sum of unsaturated aliphatic diacids	20.0	11.8	2.48	47.8	36.8	13.9	21.0	56.3	22.3	20.5	2.70	69.5
Aromatic acids (ng m^{-3})												
phthalic acid (Ph)	8.02	3.05	3.00	12.4	10.5	1.77	8.09	12.8	5.88	3.73	1.45	13.0
isophthalic acid (iPh)	10.1	5.28	0.98	21.2	11.7	6.50	6.75	20.2	5.76	3.32	1.72	11.2
benzoic acid	5.46	2.76	0.47	11.4	5.88	0.52	5.01	6.29	4.47	2.44	1.07	8.41
sum of aromatic acids	23.6	10.2	8.30	45.1	28.1	8.24	21.1	39.3	16.1	8.86	4.25	30.3
Hydroxyl- and polyacids (ng m^{-3})												
glyceric acid	2.20	1.81	0.22	6.56	3.52	1.34	2.00	4.89	2.68	1.48	0.60	5.17
malic acid	3.00	1.45	0.95	5.73	4.32	2.06	1.52	6.60	3.67	1.88	0.77	6.51
tartaric acid	0.45	0.54	0.06	1.89	1.10	0.42	0.49	1.48	1.37	0.83	0.14	2.83
sum of hydroxyl and polyacids	5.66	2.63	1.24	10.4	8.94	3.73	4.01	12.2	7.73	4.14	1.51	14.5

Lignin and resin acids (ng m^{-3})												
4HBA, 4-hydroxybenzoic acid	2.10	2.89	0.36	9.32	2.50	0.86	1.09	3.31	3.40	2.26	0.05	6.02
vanillic acid	1.12	2.05	0.00	5.96	2.50	0.98	1.23	3.53	4.76	3.36	0.02	8.98
syringic acid	28.0	40.7	0.23	97.8	0.21	0.20	0.01	0.54	1.18	2.95	0.01	8.47
dehydroabietic acid	15.3	4.80	4.30	22.7	14.4	7.91	8.22	23.4	17.0	14.0	5.45	40.9
sum of lignin and resin acids	46.5	38.0	15.8	114	19.7	8.78	10.8	29.5	26.3	15.6	9.58	56.1
α-Dicarbonyls (ng m^{-3})												
MeGly, methylglyoxal	20.4	29.2	7.47	103	10.1	4.93	6.55	18.7	6.43	3.04	2.12	10.4
Other species (μg m^{-3})												
MSA^-, methanesulfonic acid	0.09	0.02	0.06	0.12	0.04	0.01	0.02	0.05	0.02	0.01	0.00	0.03
formic acid	0.18	0.05	0.08	0.25	0.12	0.01	0.11	0.14	0.05	0.02	0.02	0.08
acetic acid	0.22	0.11	0.07	0.44	0.16	0.07	0.08	0.27	0.05	0.01	0.03	0.06

Note that: OC=organic carbon; TC=total carbon; WSOC=water-soluble OC; WISOC=water-insoluble OC. nss-Ca^{2+} refers to non-sea-salt Ca^{2+}. nd means not detected. Water-insoluble OC (WISOC) was calculated as the difference between OC and WSOC.

Table 2. Abundance and contributions of OC from primary sources (i.e., biomass burning, fungal spores, and plant debris) and from secondary formation (biogenic and anthropogenic VOCs) to OC in $PM_{2.5}$.

$PM_{2.5}$ concentration (μg m^{-3})	**>200**				**100-200**				**<100**			
	mean	std	min	max	mean	std	min	max	mean	std	min	max
Abundance (μg m^{-3})												
BB-OC	5.79	1.50	3.48	8.86	2.27	0.34	1.74	2.69	2.47	1.48	0.72	4.86
Fungal spores-OC	0.44	0.14	0.21	0.62	0.42	0.09	0.32	0.52	0.29	0.18	0.09	0.68
plant debris-OC	0.29	0.12	0.07	0.55	0.45	0.21	0.28	0.80	0.23	0.08	0.10	0.35
sum of POC	6.52	1.62	3.77	9.65	3.14	0.46	2.48	3.67	2.99	1.56	1.23	5.39
Isoprene SOC	0.03	0.03	0.003	0.09	0.04	0.01	0.02	0.05	0.03	0.02	0.01	0.07
Monoterpene SOC	0.02	0.02	0.01	0.06	0.03	0.02	0.01	0.06	0.01	0.004	0.01	0.02
Sesquiterpene SOC	0.01	0.02	0.00	0.04	0.01	0.02	0.00	0.04	0.01	0.02	0.00	0.06
sum of BSOC	0.06	0.05	0.01	0.16	0.08	0.04	0.04	0.15	0.06	0.03	0.01	0.10
Naphthalene SOC	0.21	0.08	0.08	0.32	0.27	0.05	0.21	0.33	0.15	0.10	0.04	0.34
sum of SOC	0.26	0.11	0.09	0.49	0.36	0.07	0.28	0.44	0.21	0.12	0.05	0.41
total	6.79	1.68	3.86	9.98	3.50	0.50	2.76	4.07	3.20	1.57	1.54	5.62
Contribution to OC (%)												

BB-OC	16.3	3.39	10.6	23.6	9.63	0.56	8.96	10.3	15.9	7.01	8.29	26.5
Fungal spores-OC	1.23	0.31	0.74	1.63	1.81	0.47	1.23	2.32	2.38	2.26	0.56	7.50
plant debris-OC	0.83	0.39	0.30	1.74	1.99	1.02	0.98	3.48	1.69	0.75	0.62	2.44
sum of POC	18.4	3.62	12.2	25.7	13.4	1.97	11.3	16.0	19.9	8.31	11.5	31.3
Isoprene SOC	0.07	0.08	0.01	0.25	0.18	0.08	0.07	0.24	0.23	0.18	0.04	0.60
Monoterpene SOC	0.05	0.04	0.02	0.15	0.13	0.08	0.05	0.25	0.09	0.04	0.04	0.15
Sesquiterpene SOC	0.03	0.05	0.00	0.14	0.04	0.08	0.00	0.19	0.13	0.22	0.00	0.66
sum of BSOC	0.15	0.14	0.05	0.43	0.36	0.20	0.14	0.67	0.44	0.34	0.09	1.10
naphthalene SOC	0.59	0.21	0.27	0.88	1.17	0.22	0.88	1.46	1.12	0.84	0.29	2.46
sum of SOC	0.74	0.29	0.38	1.28	1.53	0.37	1.01	1.99	1.57	1.13	0.38	3.56
total	19.1	3.74	12.8	26.6	15.0	2.28	12.6	17.8	21.5	8.29	11.9	32.2

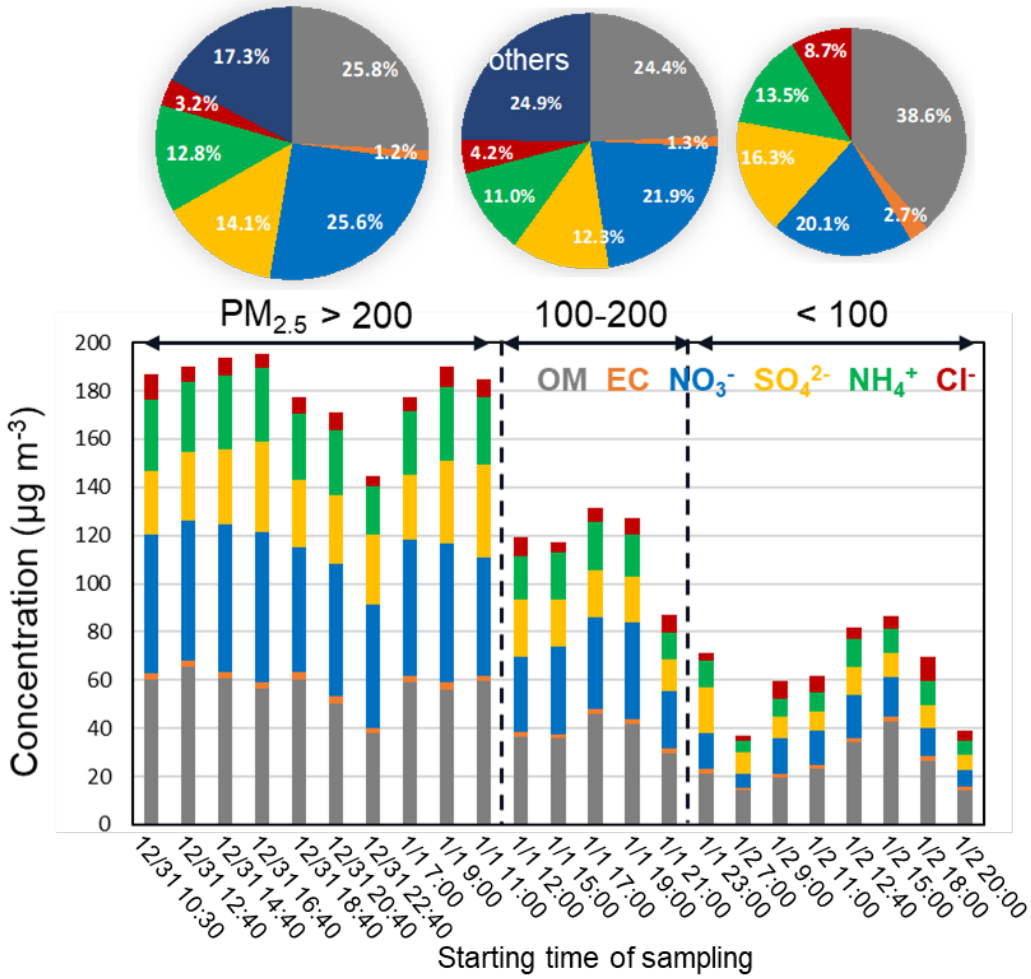

Figure 1. Temporal variations of dominant $PM_{2.5}$ compositions based on different $PM_{2.5}$ levels (i.e., <100, 100-200, and >200 μg m^{-3}). The concentrations of organics (OM) were derived from OC concentration by multiplying it by a recommended factor of 1.6 (Turpin et al., 2001). Others represent the fine particles removing the organics, secondary inorganic aerosol (sulfate, nitrate, ammonium） and chloride. The pie charts present the average contribution of major components to $PM_{2.5}$ during three pollution episodes.

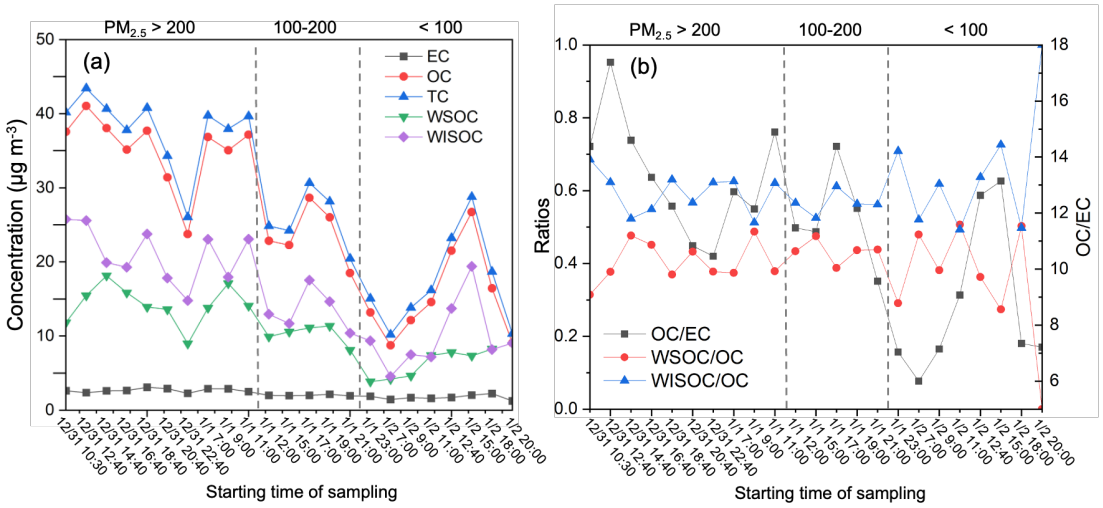

Figure 2. (a) Temporal variations of OC (organic carbon), EC (elemental carbon), WSOC (water-soluble organic carbon), WISOC (water-insoluble organic carbon), total carbon (TC) (units are μg m^{-3}), and (b) the ratios of OC/EC, WSOC/OC, and WISOC/OC in $PM_{2.5}$ samples in Nanjing.

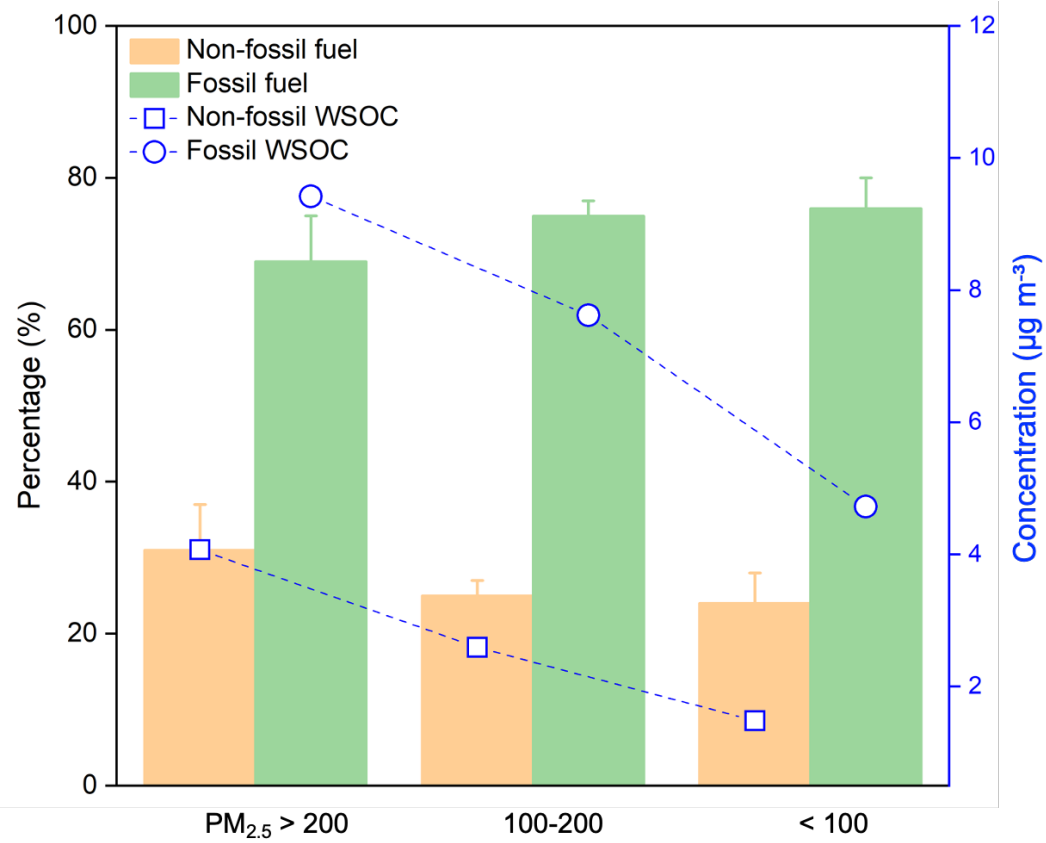

Figure 3. Comparison of fossil and non-fossil source contributions to water-soluble organic carbon (WSOC) in urban $PM_{2.5}$ samples during three haze episodes (i.e., $PM_{2.5}$ > 200, 100-200, and < 100 μg m^{-3}).

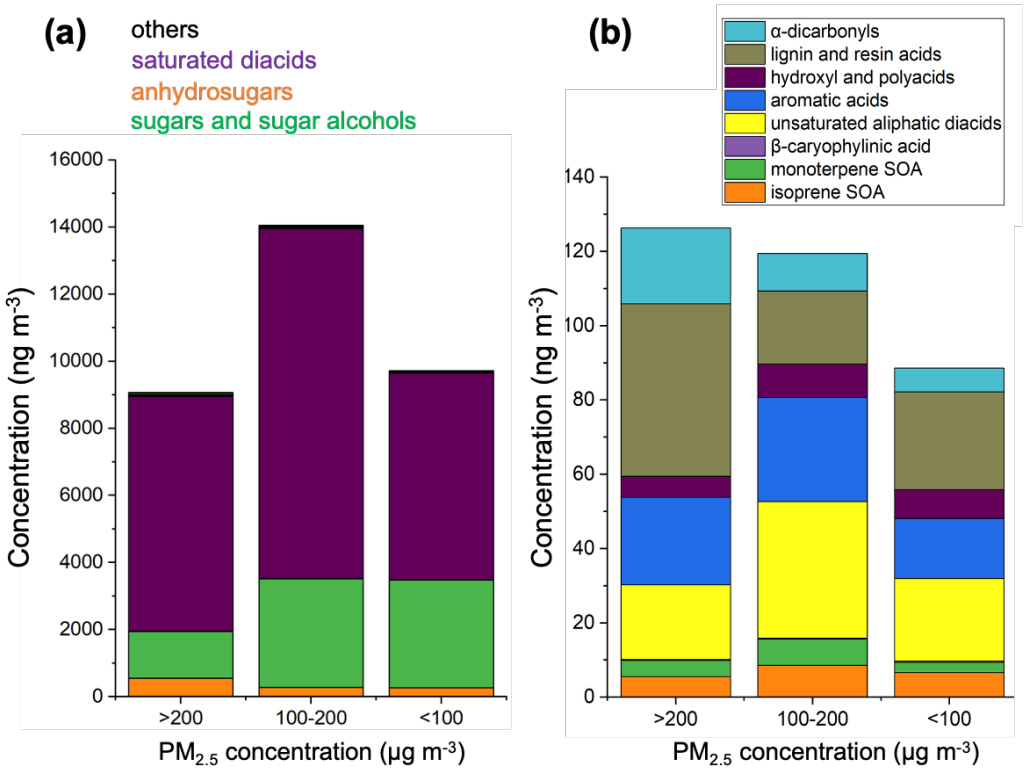

Figure 4. Average concentrations of measured carbonaceous species during three episodes with $PM_{2.5}$ levels in the ranges of > 200, 100-200, and < 100 μg m^{-3}, respectively. "others" in (a) denotes the sum of the components presented in (b).

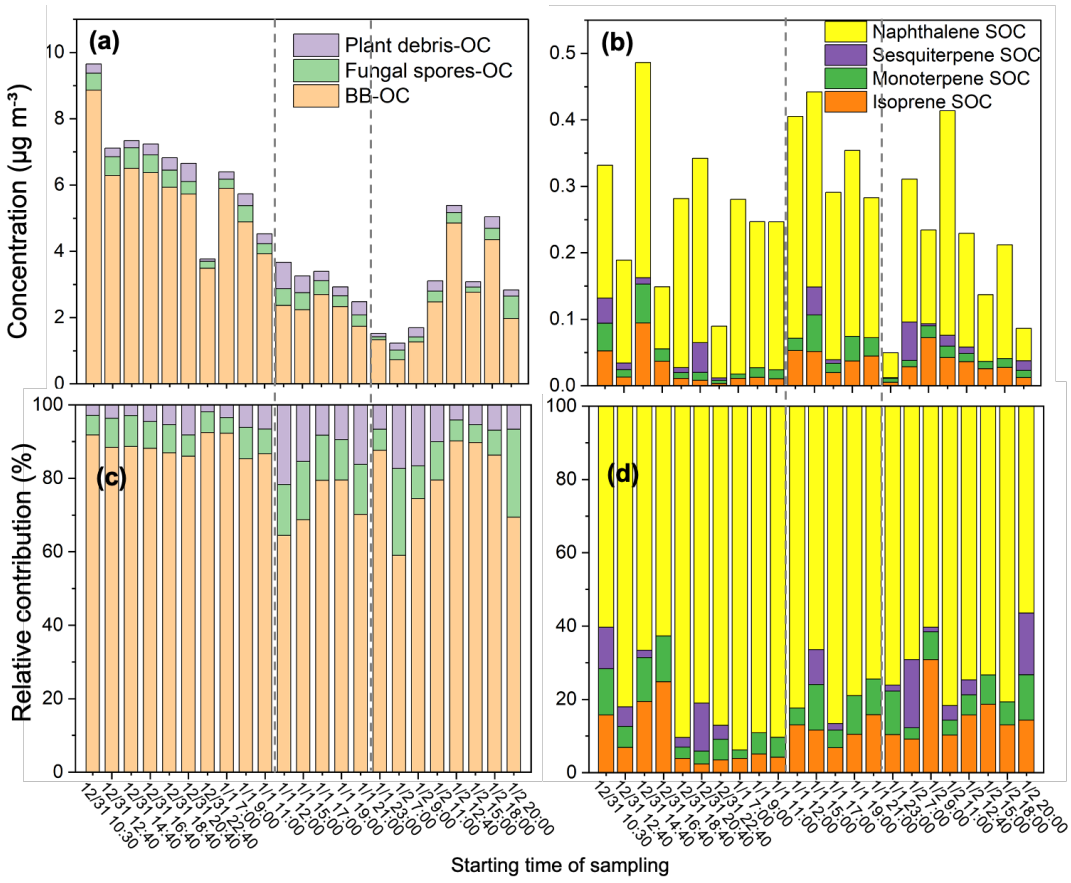

Figure 5. Concentrations of (a) primary organic carbon (OC) derived from biomass burning, fungal spores, and plant debris, and (b) secondary OC generated by isoprene, monoterpene, sesquiterpene, and naphthalene, and relative contribution of these OCs (c and d).

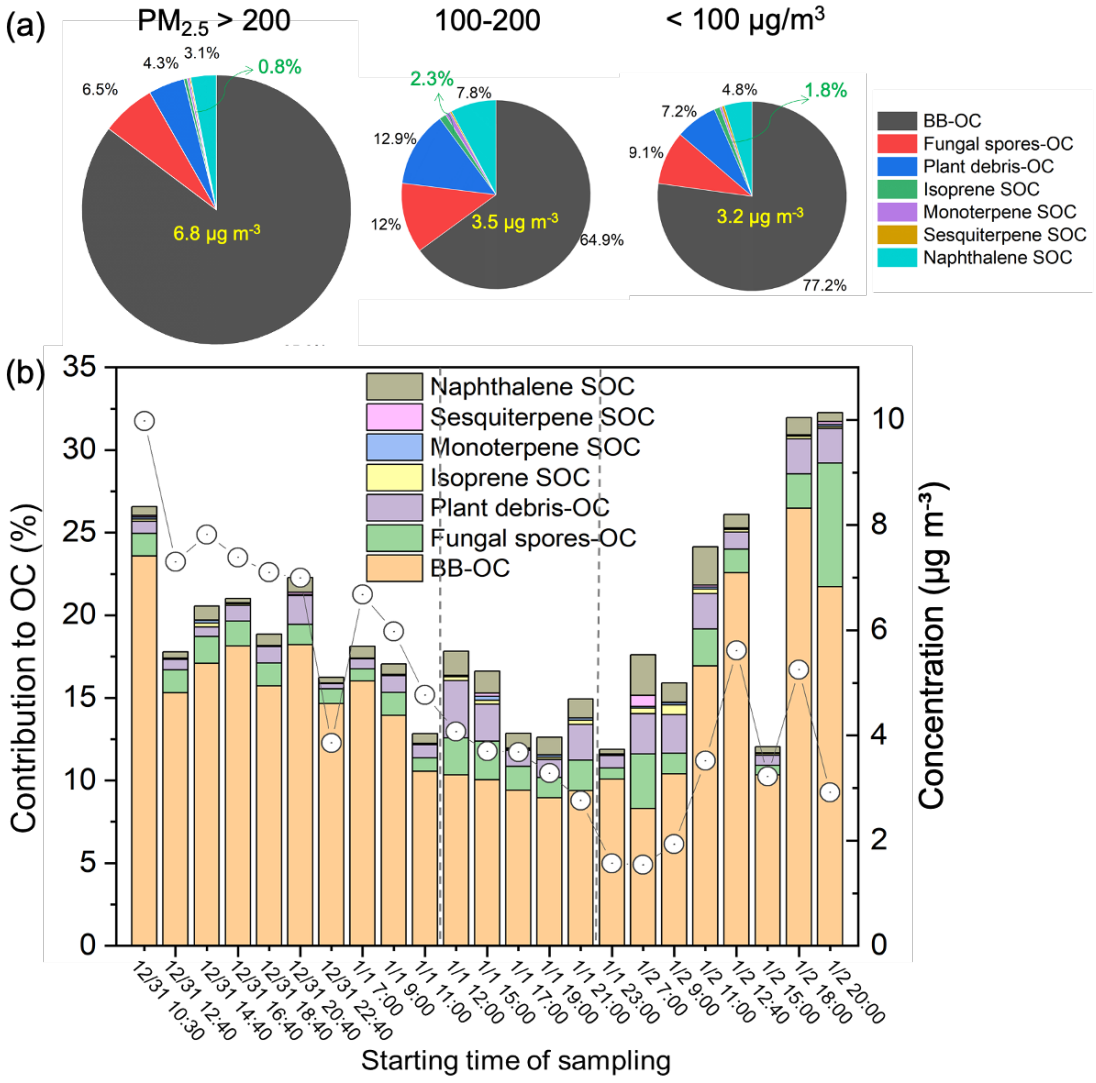

Figure 6. (a) Episode-averaged relative contributions of OC derived from biomass burning, fungal spores, plant debris, isoprene, monoterpene, sesquiterpene, and naphthalene to OC in $PM_{2.5}$ (%). The yellow numbers refer to the total tracer-based OC concentrations attributed to these sources (μg m^{-3}). Each pie size is proportional to its total tracer-based OC concentration. The green arrows and numbers represent the biogenic SOC fraction contributed by isoprene, monoterpene, and sesquiterpene. (b) Contributions of biomass burning, fungal spores, plant debris, isoprene, monoterpene, sesquiterpene, and naphthalene to OC in $PM_{2.5}$ (%), and OC concentrations attributed to these sources (μg m^{-3}, white circles).